

Organics

The organic contaminants in sediments tended to display a high degree of spatial heterogeneity. High contaminant concentrations were observed in sediments from a number of regions, but few trends were observed between the results of the 1982 and the 1989 studies. Of the 12 PNAs that were compared, only one (fluoranthene) displayed an overall trend throughout the study area. This PNA displayed a significant ($p=0.05$) increase of 2,000 $\mu\text{g}/\text{kg}$ between the 1979 and the 1989 data sets. This may be important because fluoranthene is the dominant PNA in most of the Elizabeth River sediments (Alden and Hall, 1984; Alden and Butt, 1988). However, caution should be exercised in the interpretation of a single "significant" result from so many comparisons, when chance alone could be responsible (i.e. there is a fair probability, that, of the 13 statistical tests run on the organics data, one would be significant at the 0.05 level).

The total PNAs in sediments did not differ significantly ($p=0.80$) between 1982 (grand mean = 35,600 $\mu\text{g}/\text{kg}$) and 1989 (grand mean = 43,300 $\mu\text{g}/\text{kg}$). However, the samples from several regions appeared to display major changes (Figs. 44, 45). The total PNAs in sediments appeared to decrease at Site J, and increase at the Site K shoals. The greatest apparent increase was in the Site O channel sample. Of course, single sample comparisons are subject to variation due to small scale patchiness (i.e. small globs of creosote could be seen in the Site O samples). However, Site O is

Figure 44. Change in total PNA concentrations in Elizabeth River sediments from 1982 to 1989.

CHANGE IN TOTAL PNA CONCENTRATIONS IN SEDIMENTS FROM 1982 TO 1989

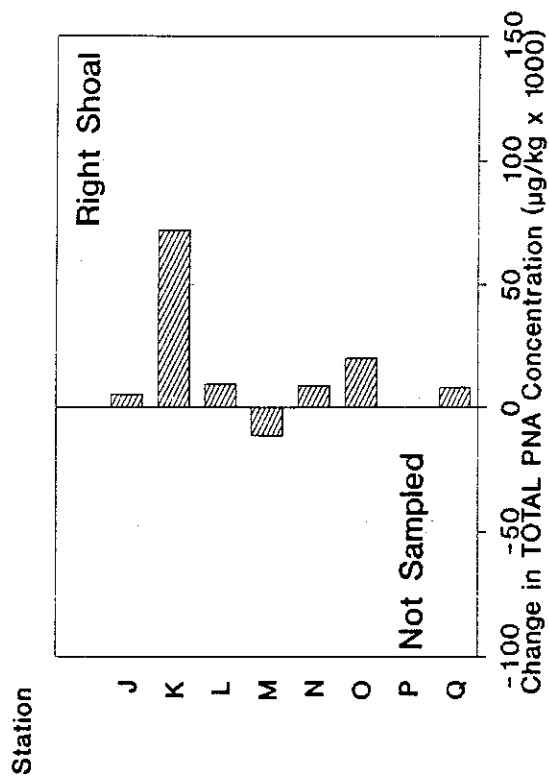
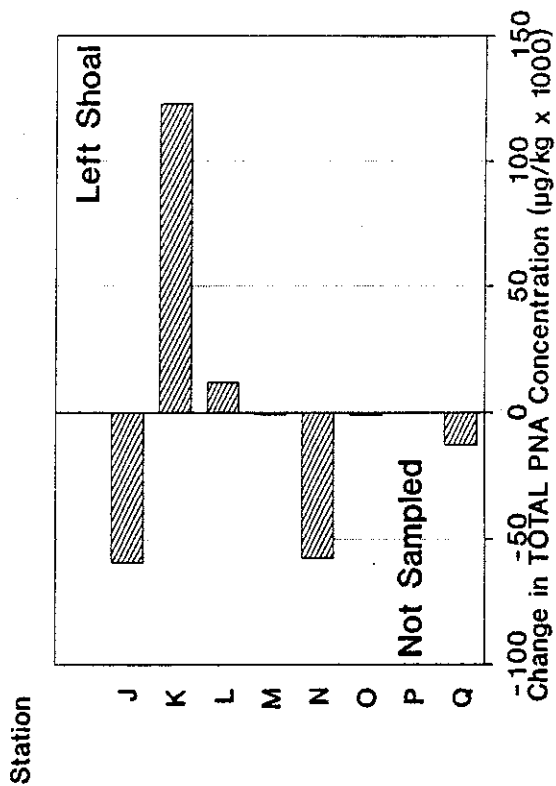
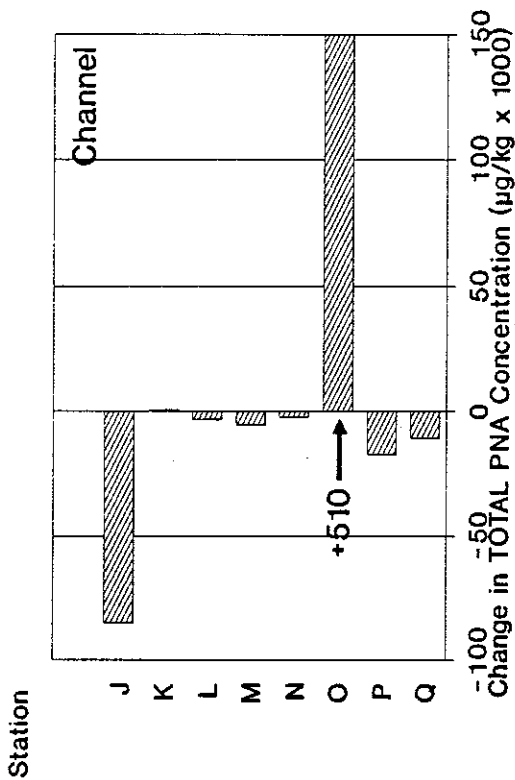
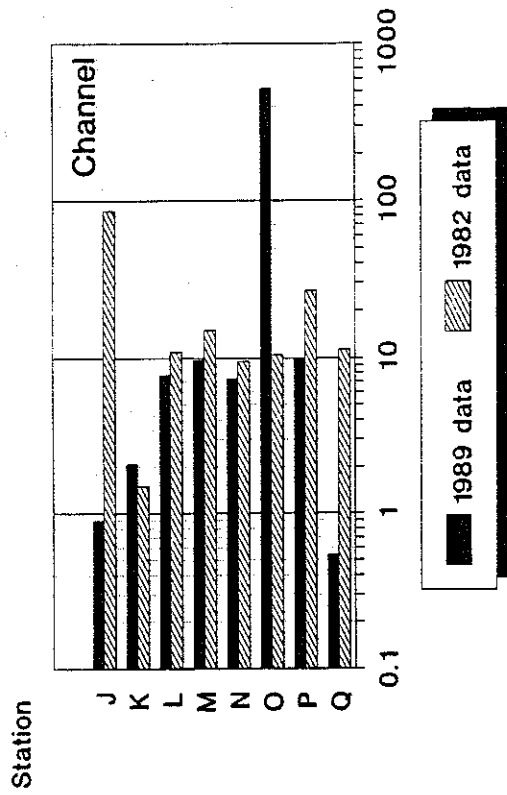
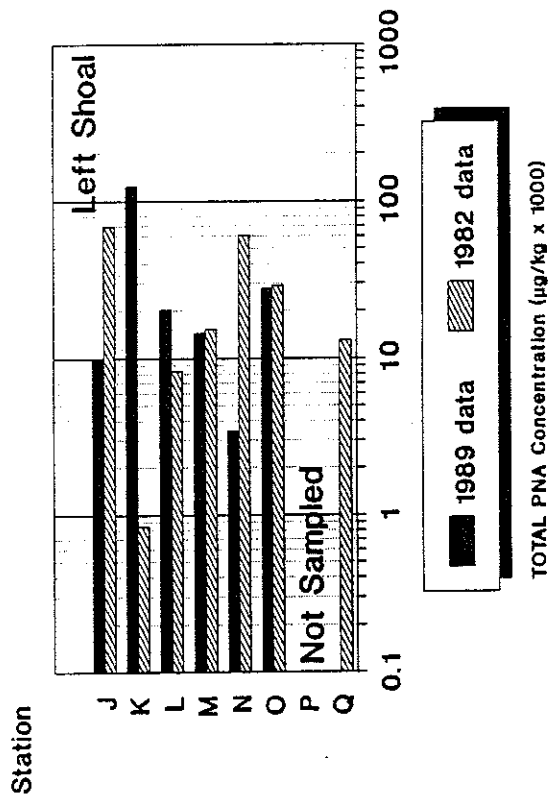


Figure 45. Comparison of total PNA concentrations in Elizabeth River sediments between 1982 and 1989.

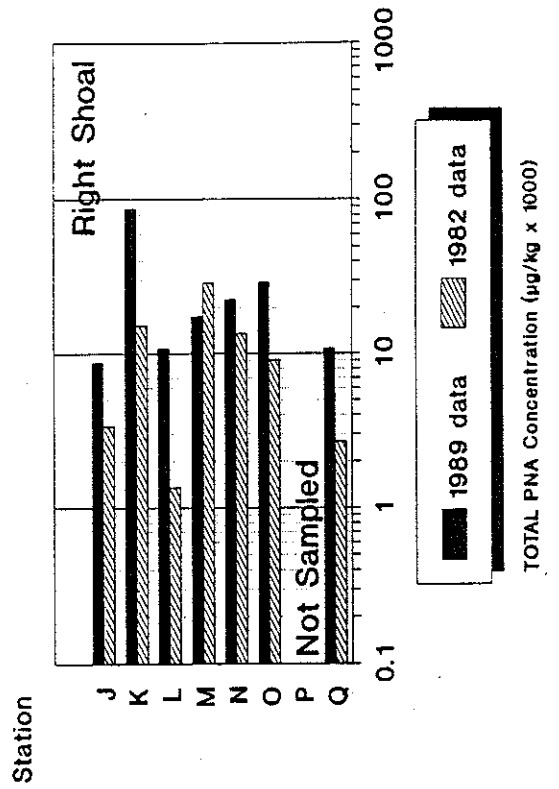
TOTAL PNAs in Elizabeth River Sediments



TOTAL PNAs in Elizabeth River Sediments



TOTAL PNAs in Elizabeth River Sediments



1
2
3
4
5
6
7
8
9
10
11
12
13
14
15
16
17
18
19
20
21
22
23
24
25
26
27
28
29
30
31
32
33
34
35
36
37
38
39
40
41
42
43
44
45
46
47
48
49
50
51
52
53
54
55
56
57
58
59
60
61
62
63
64
65
66
67
68
69
70
71
72
73
74
75
76
77
78
79
80
81
82
83
84
85
86
87
88
89
90
91
92
93
94
95
96
97
98
99
100

in the vicinity of the abandoned Eppinger and Russell creosote factory and has been reported as being among the most contaminated regions of the Elizabeth River (Alden and Hall, 1984). It is possible that creosote from the factory site is still accumulating in the deeper channel areas due to slumping of sediments from the shoal areas. The depth distribution of total PNAs (Fig. 44) tended to confirm these apparent temporal patterns: concentrations at Site J (right shoal and channel) increased with depth; PNA concentrations at Site K were higher in the more recent surface sediments; and the Site O channel sediments displayed much higher concentrations in the 0-30 cm depth interval than in the 30-70 cm interval. Even the apparent increase in PNA concentrations in the right shoal sediments of Site O between 1982 and 1989 is reflected by a higher concentration in the surface layer (0-10 cm) than in the next depth interval (10-30 cm), although much higher concentrations were observed at greater depths (30-70 cm and 70-150 cm).

Among the 2- and 3-ring PNAs, a number of common spatio-temporal patterns have emerged. Samples from Sites J and O and the shoals of Sites M and N tended to decrease, while samples from Site K shoals tended to increase in concentrations of acenaphthalene (Figs 46 and 47), naphthalene (Figs. 48 and 49), phenanthrene (Figs. 50 and 51), anthracene (Figs. 52 and 53), and fluorene (Figs. 54 and 55). The higher molecular weight PNAs decreased at Site J and increased at Site K for fluoranthene (Figs. 56 and 57), pyrene (Figs. 58 and 59), benzo(a)anthracene (Figs. 60 and 61),

Figure 46. Change in acenaphthalene concentrations in Elizabeth River sediments from 1982 to 1989.

CHANGE IN ACENAPHTHALENE CONCENTRATIONS IN SEDIMENTS FROM 1982 TO 1989

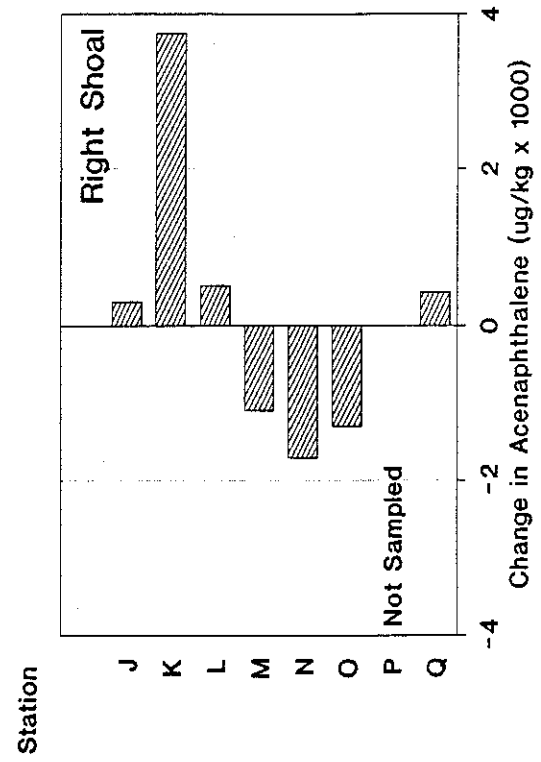
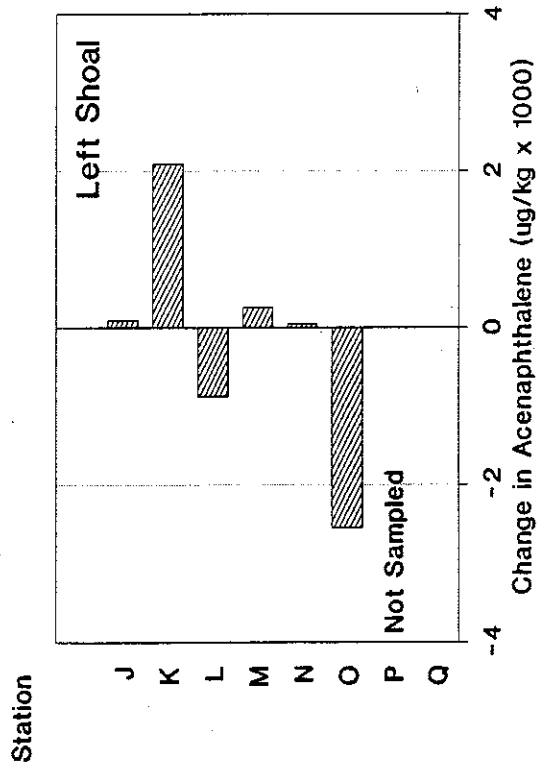
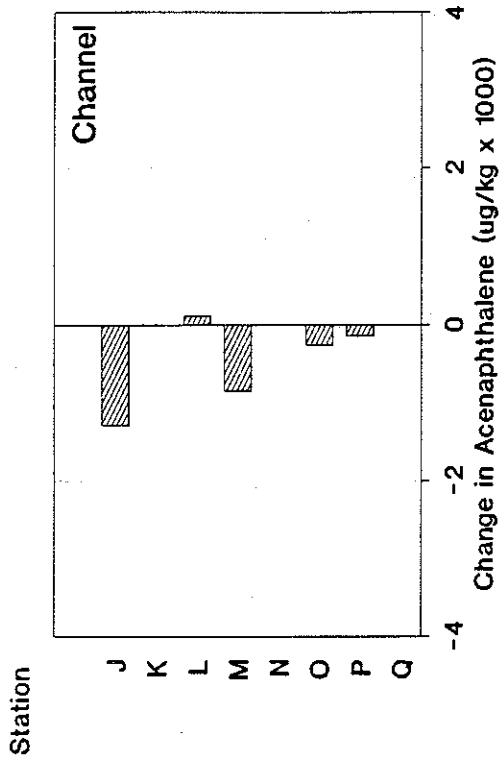
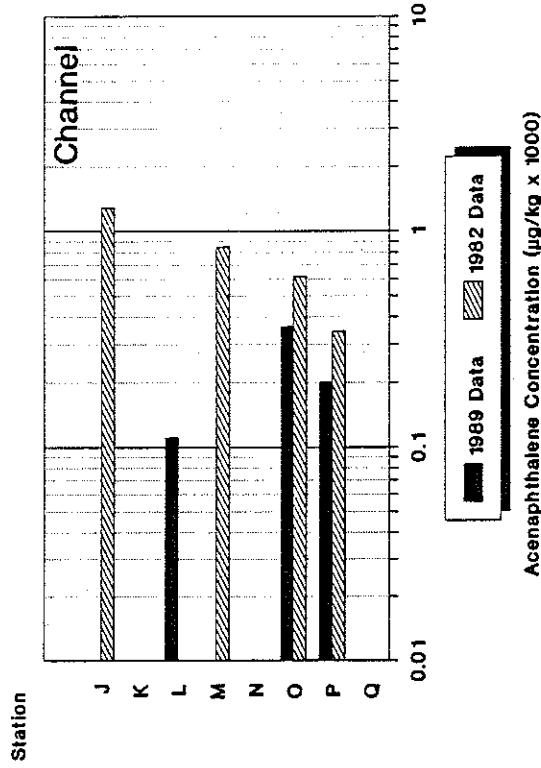
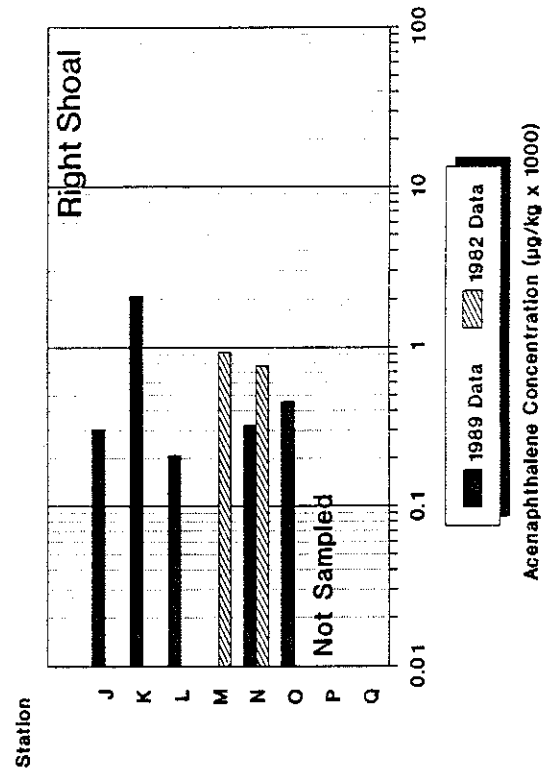


Figure 47. Comparison of acenaphthalene concentrations in Elizabeth River sediments between 1982 and 1989.

Acenaphthalene in Elizabeth River Sediments



Acenaphthalene in Elizabeth River Sediments



Acenaphthalene in Elizabeth River Sediments

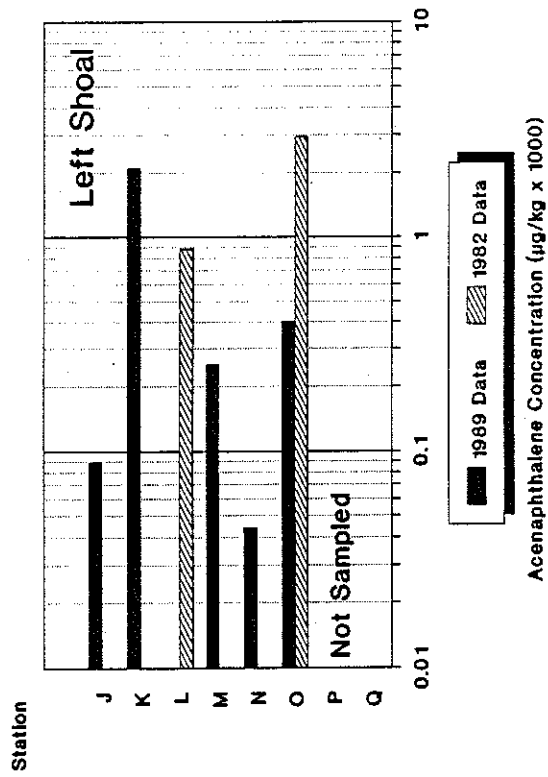
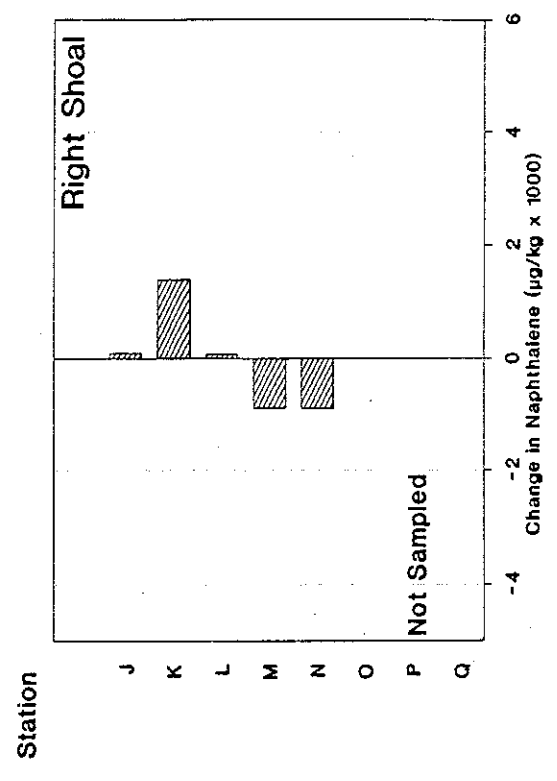
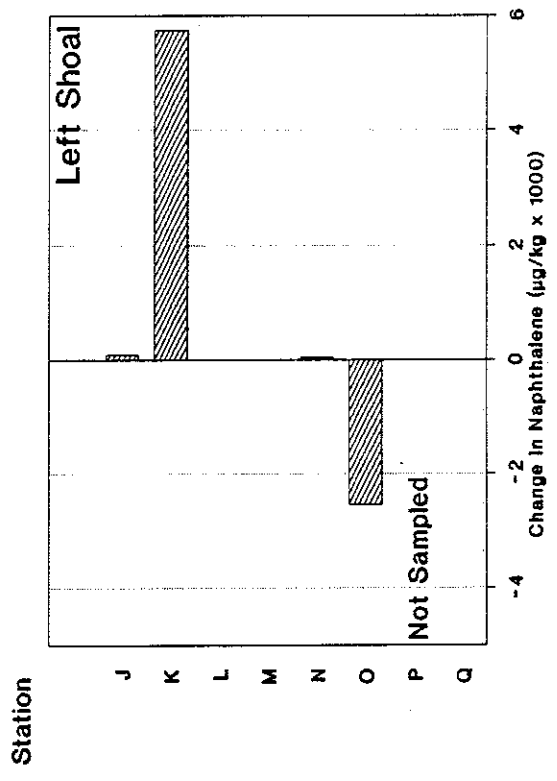
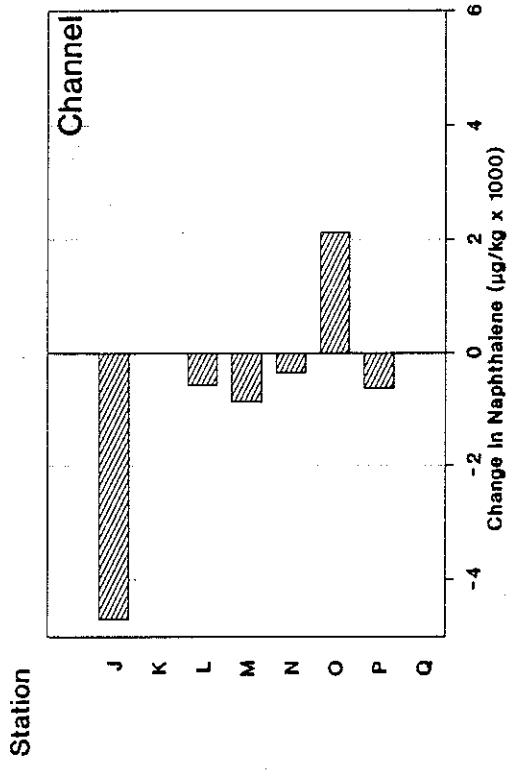


Figure 48. Change in naphthalene concentrations in Elizabeth River sediments from 1982 to 1989.

CHANGE IN NAPHTHALENE CONCENTRATIONS IN SEDIMENTS FROM 1982 TO 1989

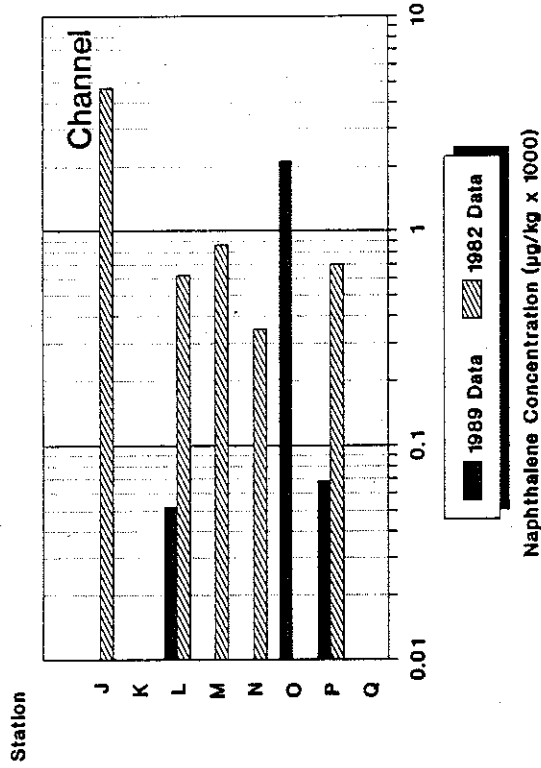


Not Sampled

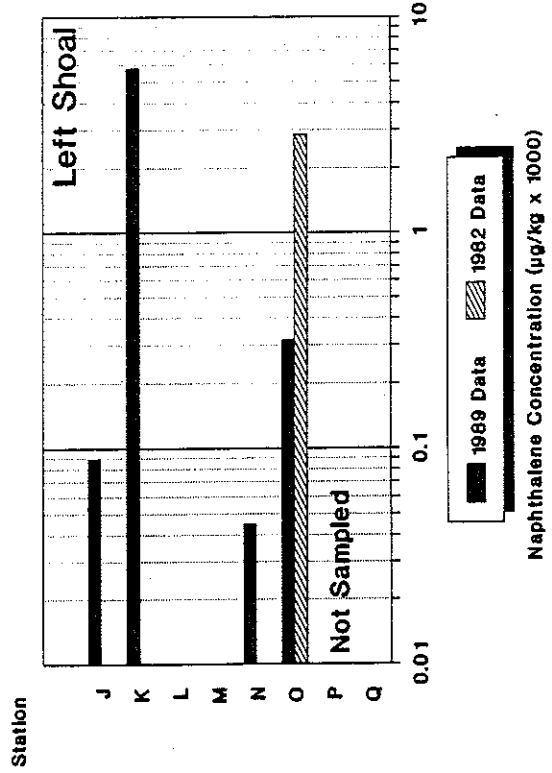
Not Sampled

Figure 49. Comparison of naphthalene concentrations in Elizabeth River sediments between 1982 and 1989.

Naphthalene in Elizabeth River Sediments



Naphthalene in Elizabeth River Sediments



Naphthalene in Elizabeth River Sediments

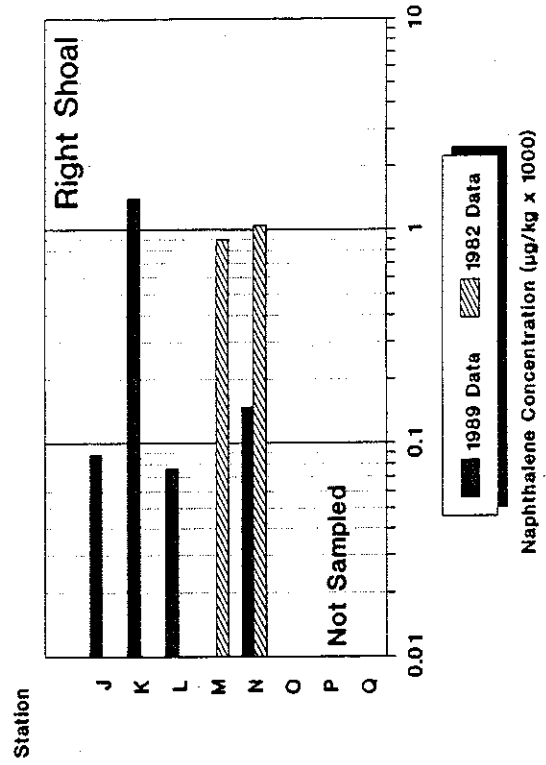


Figure 50. Change in phenanthrene concentrations in Elizabeth River sediments from 1982 to 1989.

CHANGE IN PHENANTHRENE CONCENTRATIONS IN SEDIMENTS FROM 1982 TO 1989

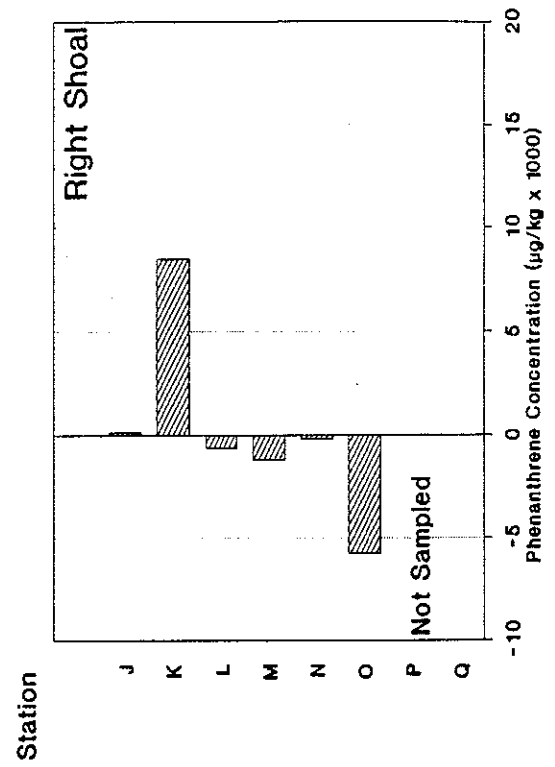
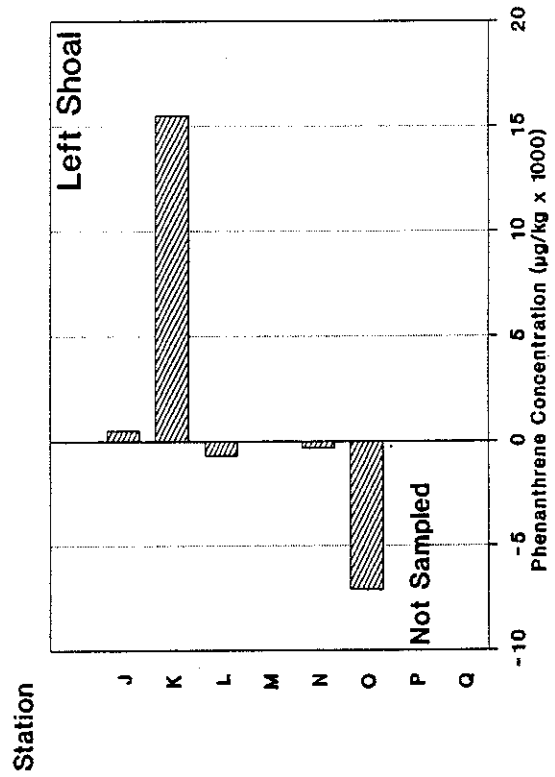
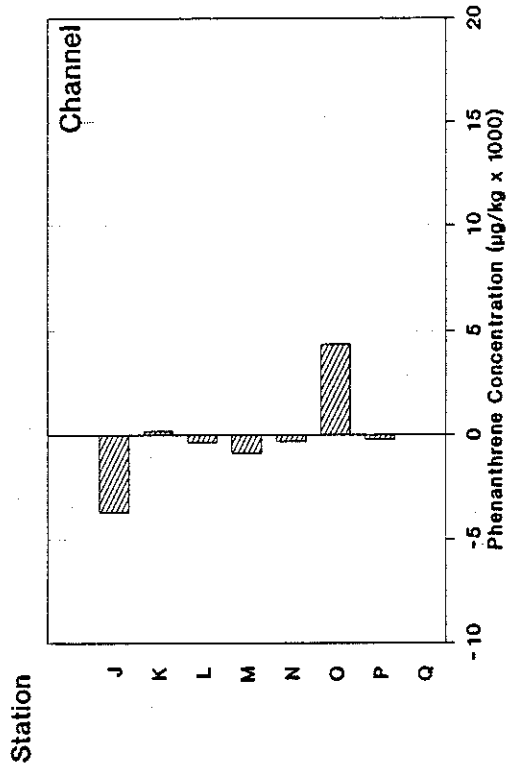
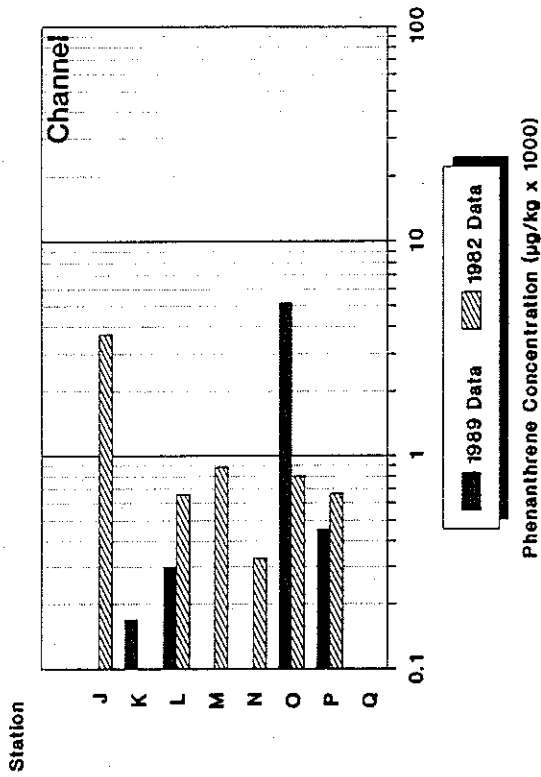
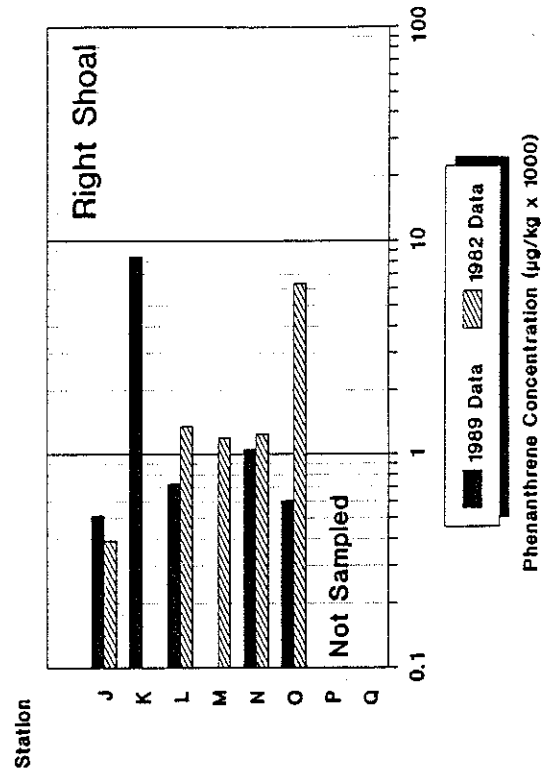


Figure 51. Comparison of phenanthrene concentrations in Elizabeth River sediments between 1982 and 1989.

Phenanthrene in Elizabeth River Sediments



Phenanthrene in Elizabeth River Sediments



Phenanthrene in Elizabeth River Sediments

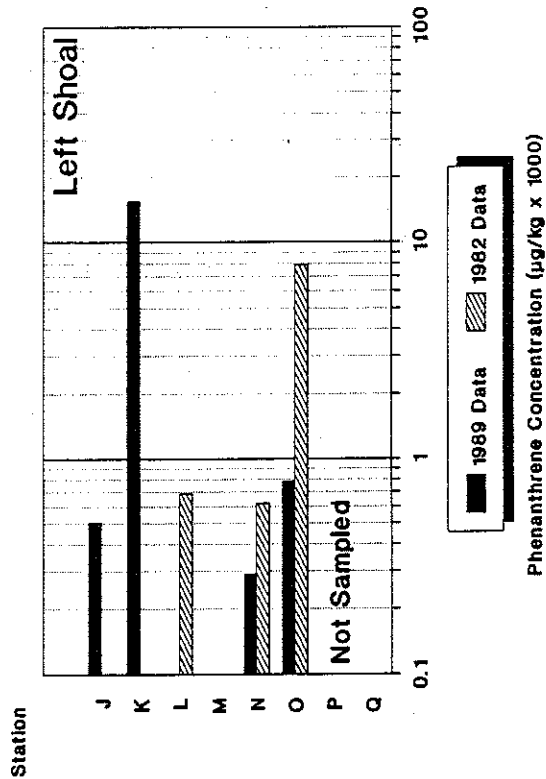


Figure 52. Change in anthracene concentrations in Elizabeth River sediments from 1982 to 1989.

CHANGE IN ANTHRACENE CONCENTRATIONS IN SEDIMENTS FROM 1982 TO 1989

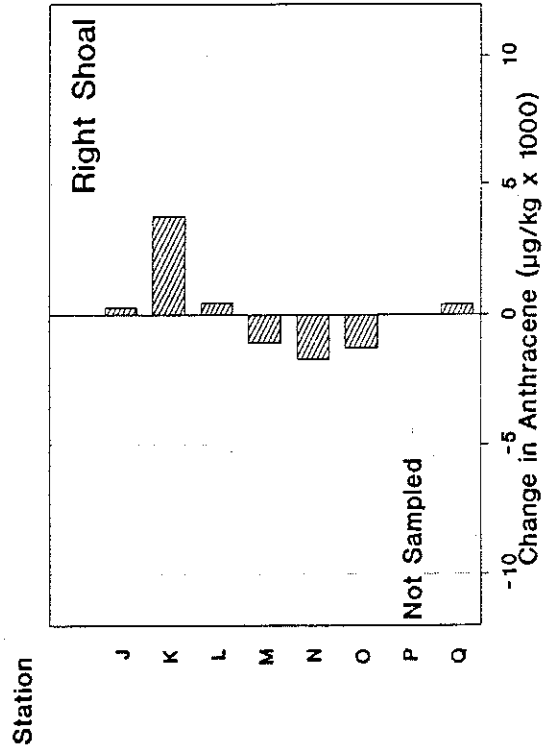
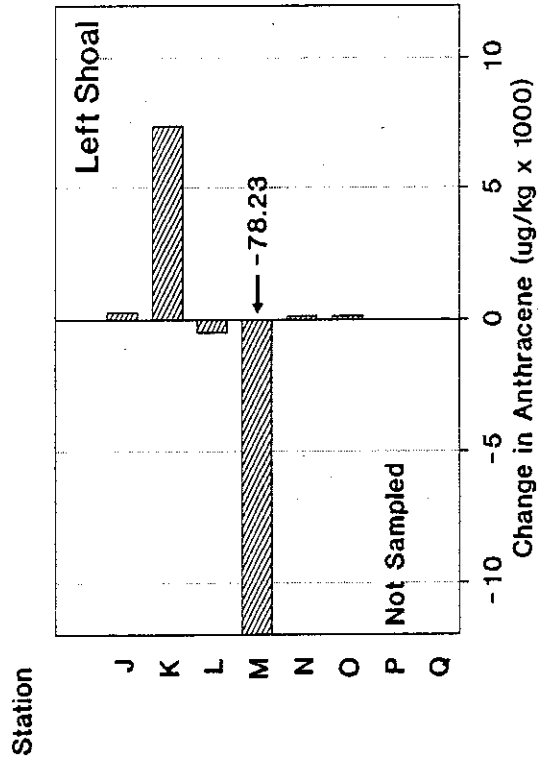
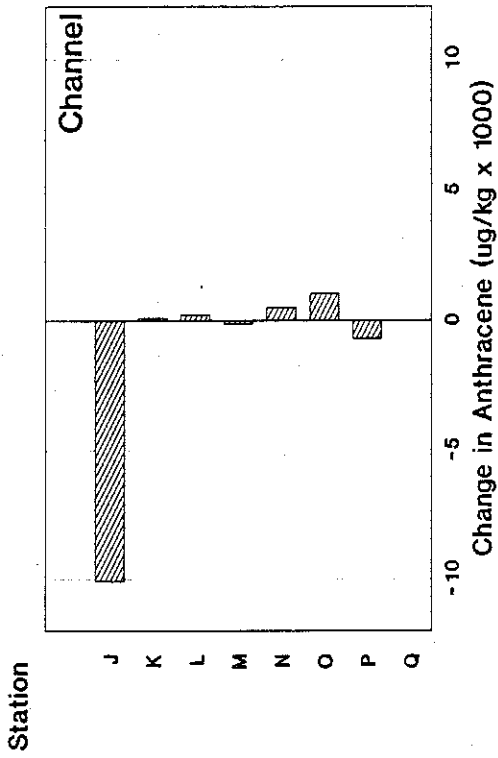
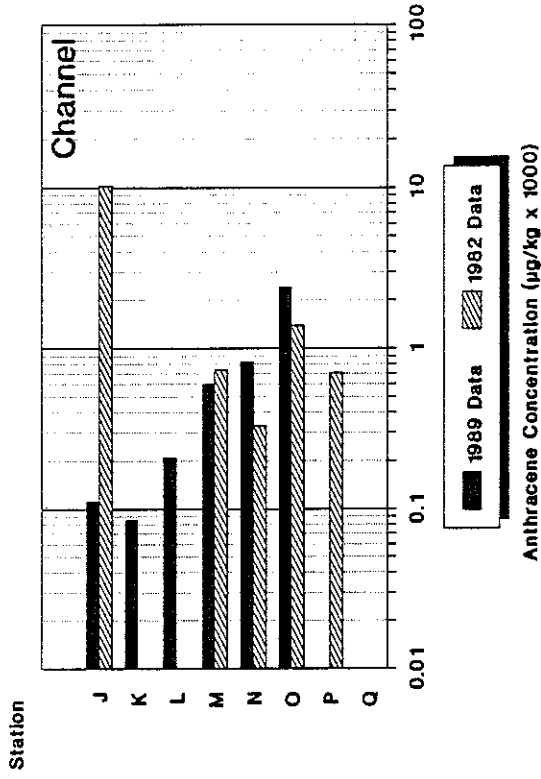
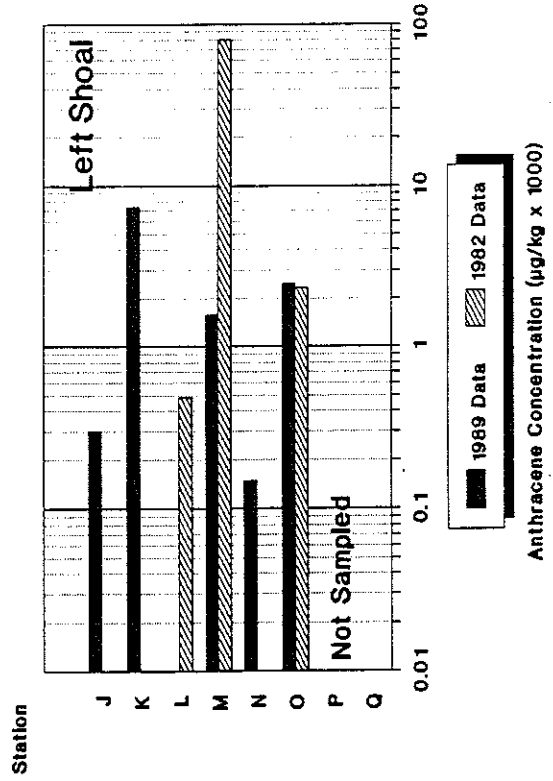


Figure 53. Comparison of anthracene concentrations in Elizabeth River sediments between 1982 and 1989.

Anthracene in Elizabeth River Sediments



Anthracene in Elizabeth River Sediments



Anthracene in Elizabeth River Sediments

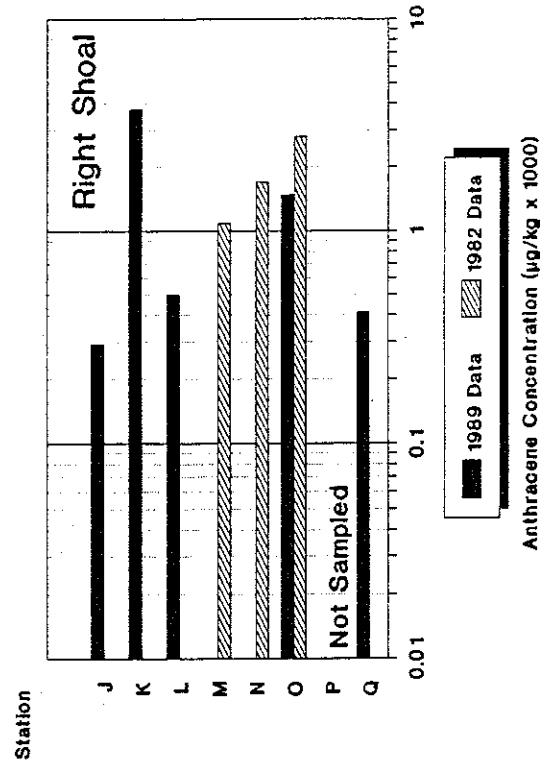


Figure 54. Change in fluorene concentrations in Elizabeth River sediments from 1982 to 1989.

CHANGE IN FLUORENE CONCENTRATIONS IN SEDIMENTS FROM 1982 TO 1989

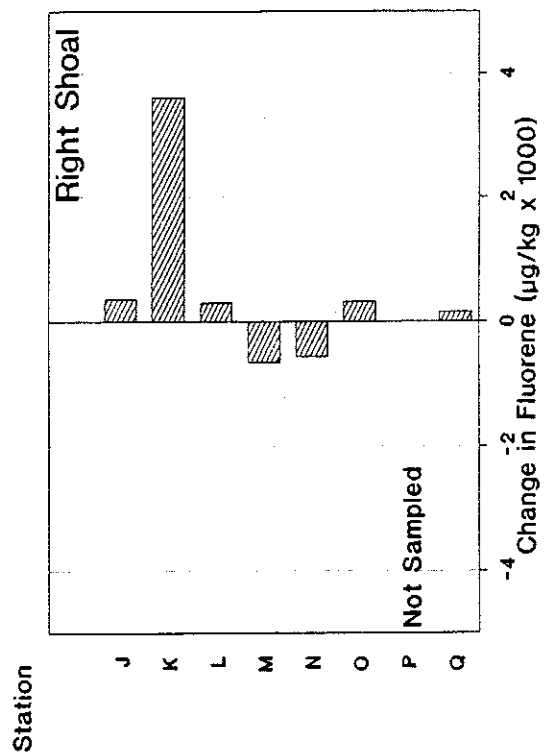
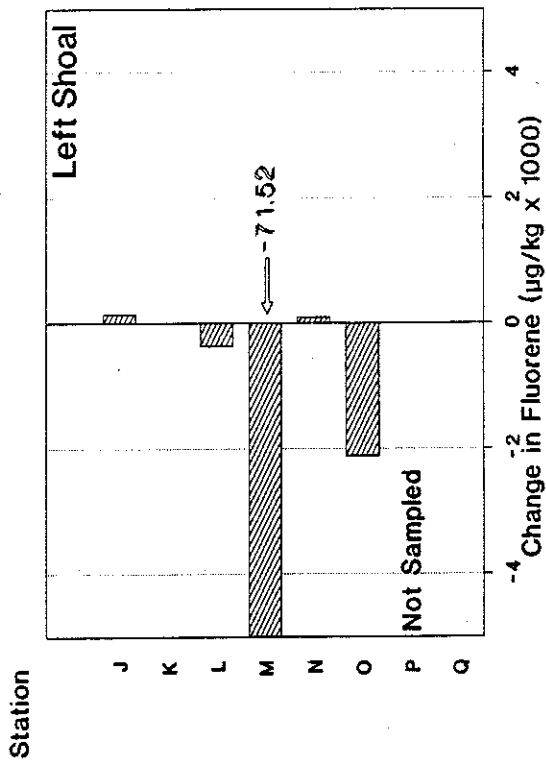
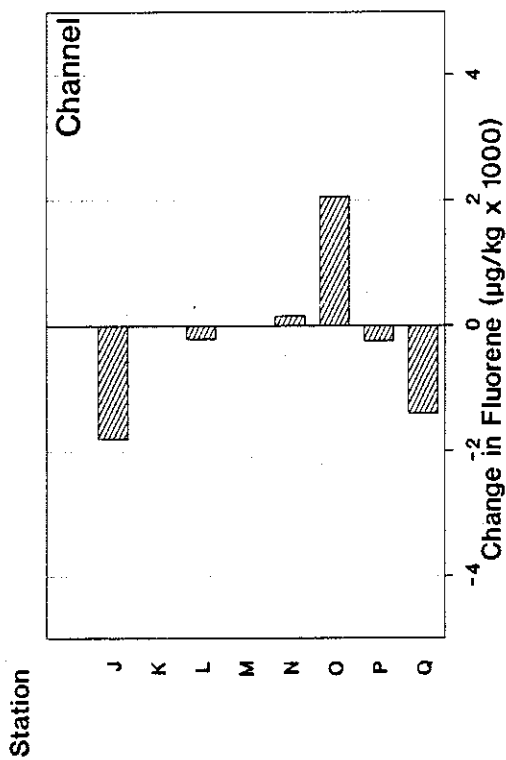
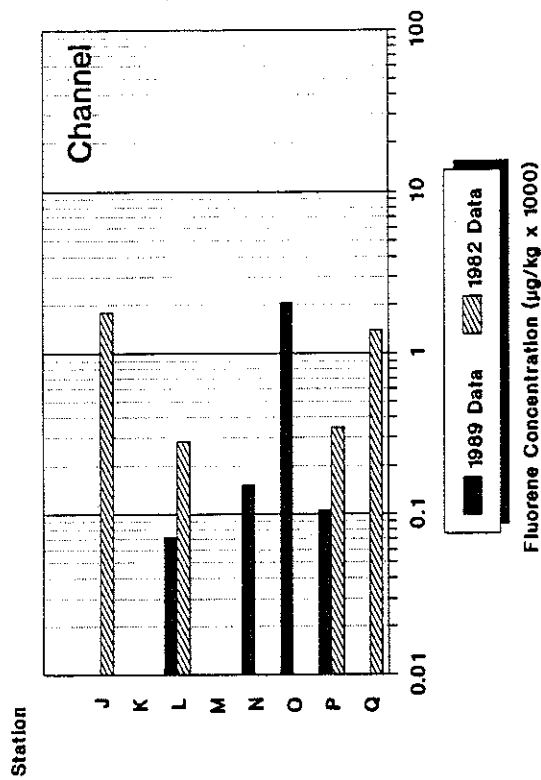
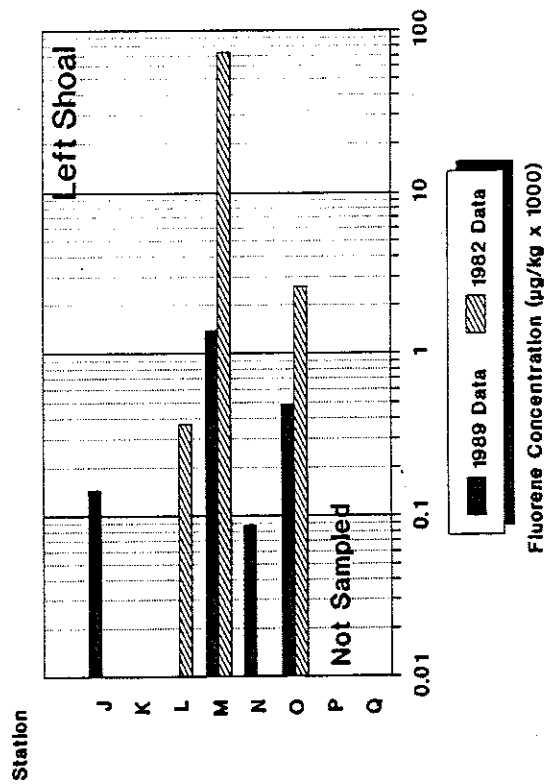


Figure 55. Comparison of fluorene concentrations in Elizabeth River sediments between 1982 and 1989.

Fluorene in Elizabeth River Sediments



Fluorene in Elizabeth River Sediments



Fluorene in Elizabeth River Sediments

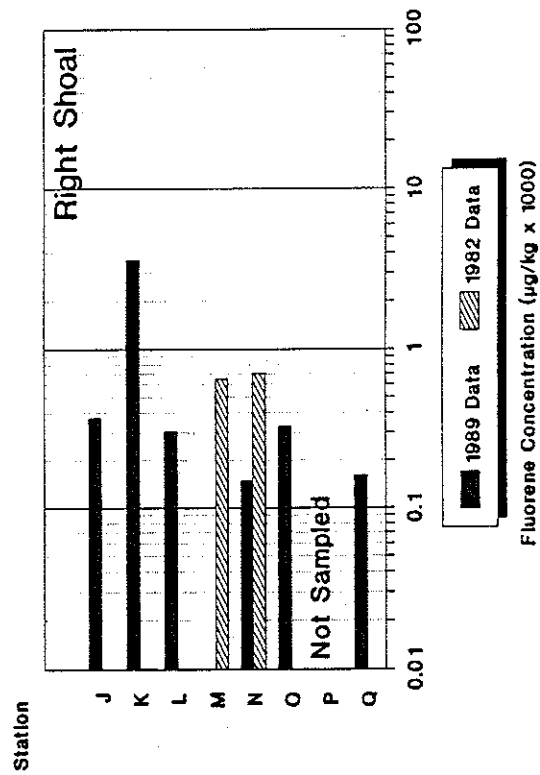


Figure 56. Change in fluoranthene concentrations in Elizabeth River sediments from 1982 to 1989.

CHANGE IN FLUORANTHENE CONCENTRATIONS IN SEDIMENTS FROM 1982 TO 1989

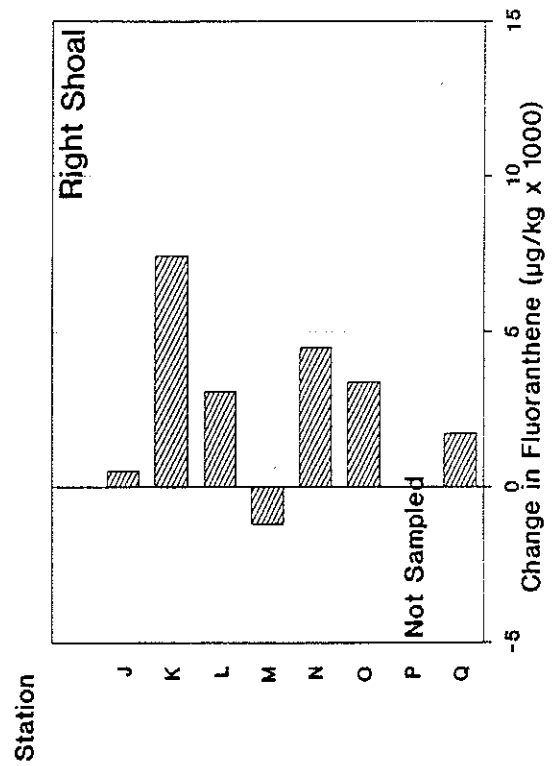
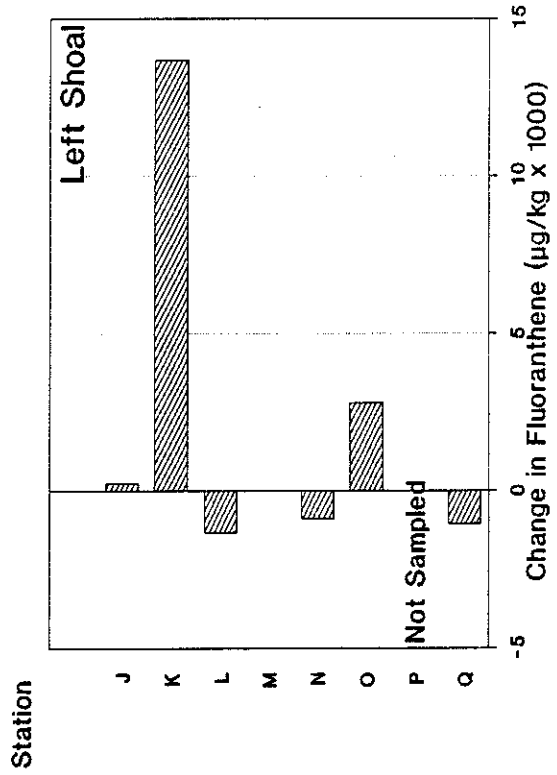
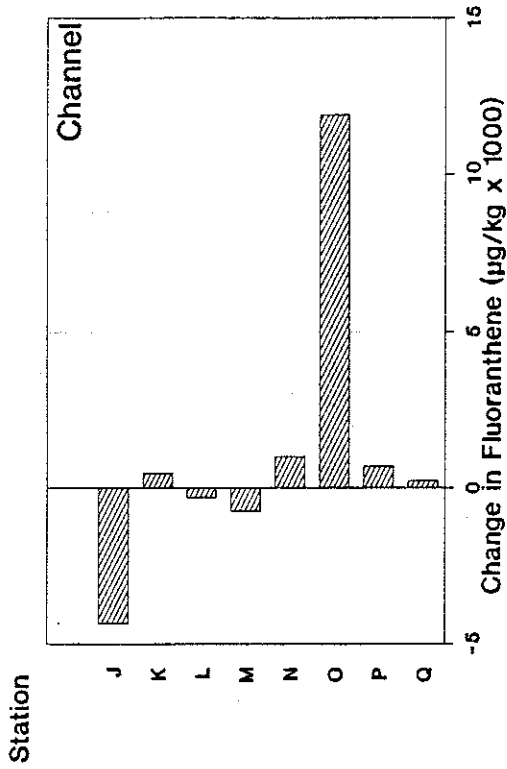
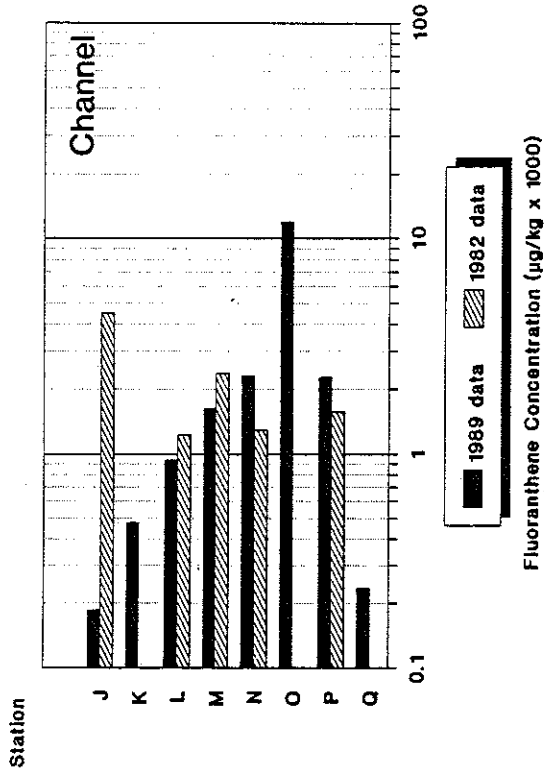
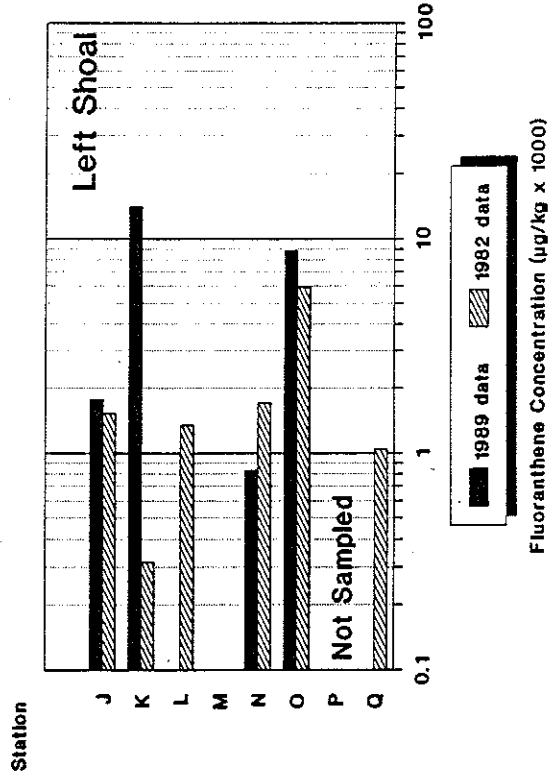


Figure 57. Comparison of fluoranthene concentrations in Elizabeth River sediments between 1982 and 1989.

Fluoranthene in Elizabeth River Sediments



Fluoranthene in Elizabeth River Sediments



Fluoranthene in Elizabeth River Sediments

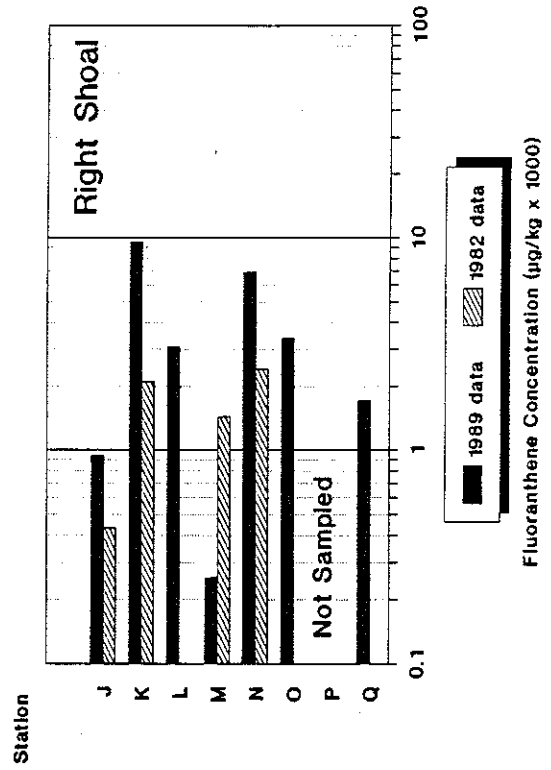


Figure 58. Change in pyrene concentrations in Elizabeth River sediments from 1982 to 1989.

CHANGE IN PYRENE CONCENTRATIONS IN SEDIMENTS FROM 1982 TO 1989

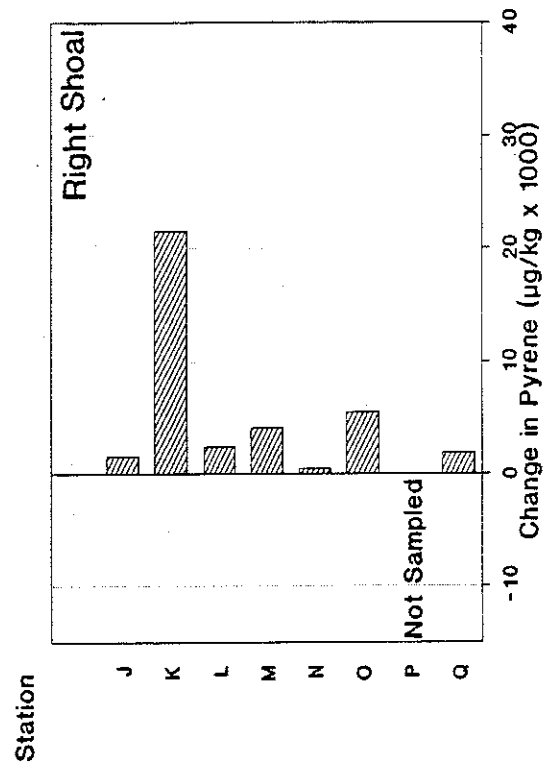
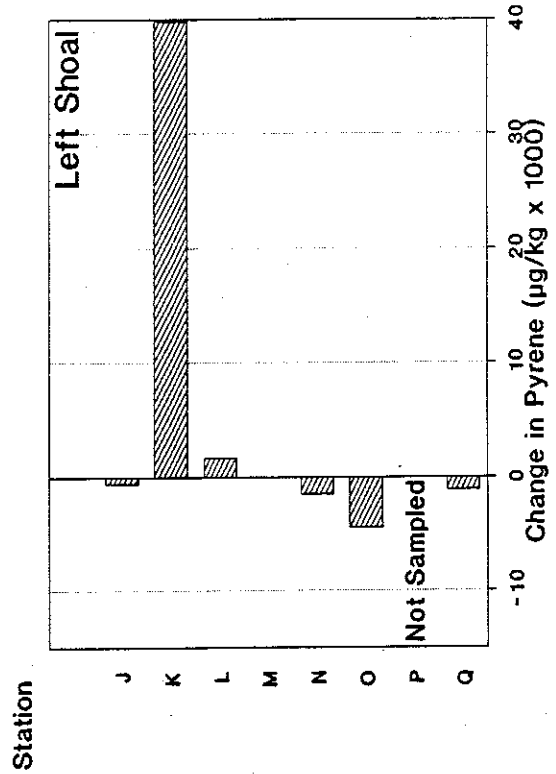
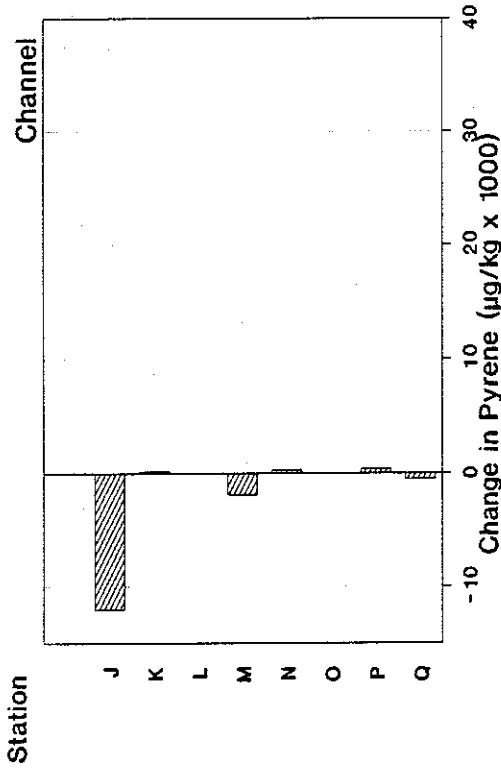
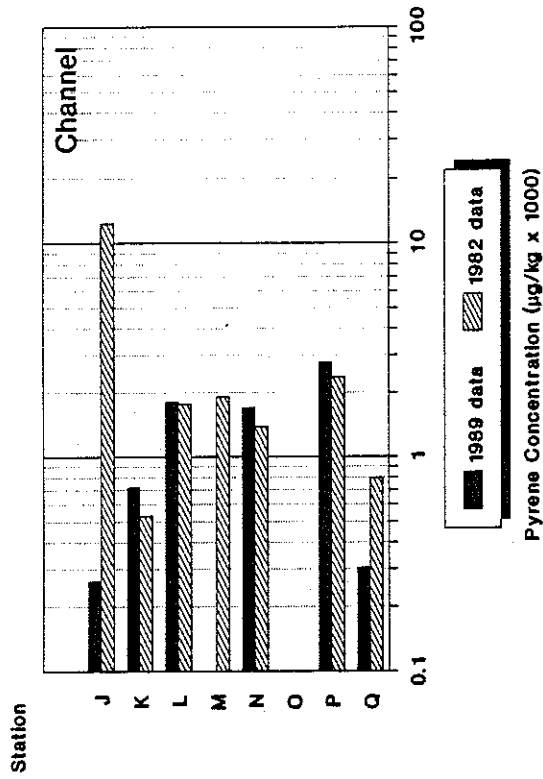
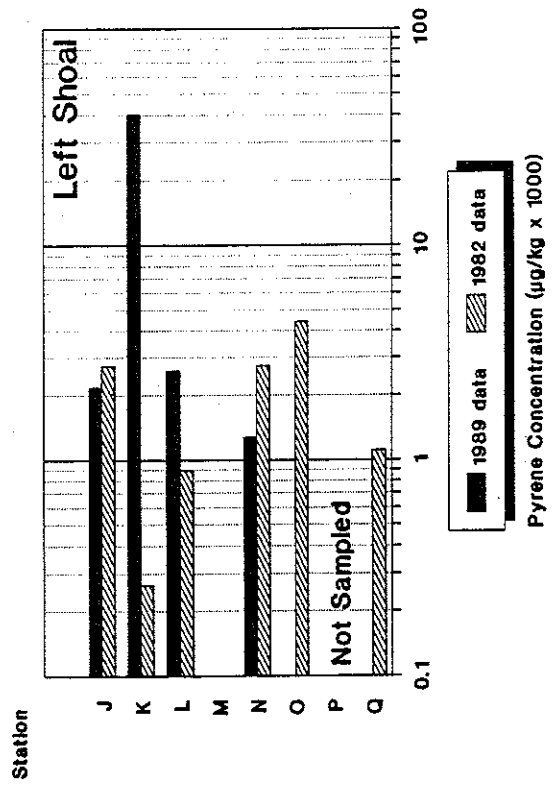


Figure 59. Comparison of pyrene concentrations in Elizabeth River sediments between 1982 and 1989.

Pyrene in Elizabeth River Sediments



Pyrene in Elizabeth River Sediments



Pyrene in Elizabeth River Sediments

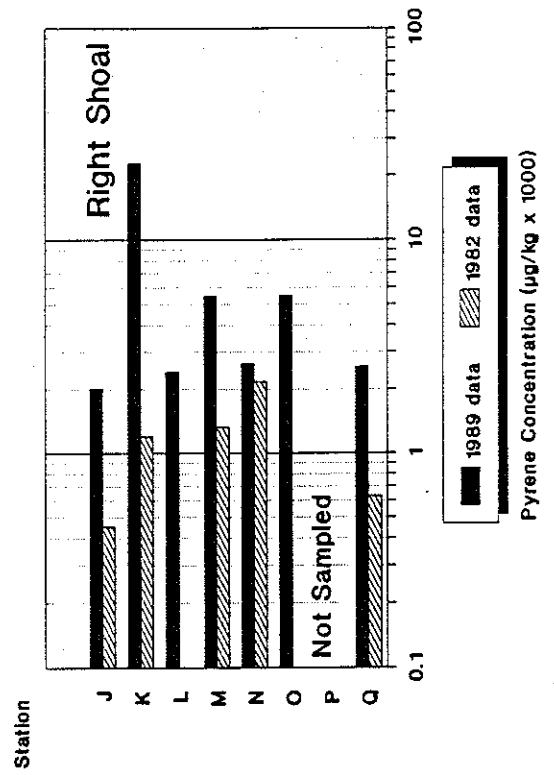


Figure 60. Change in benzo(a)anthracene concentrations in Elizabeth River sediments from 1982 to 1989.

CHANGE IN BENZO(a)ANTHRACENE
CONCENTRATIONS
IN SEDIMENTS FROM 1982 TO 1989

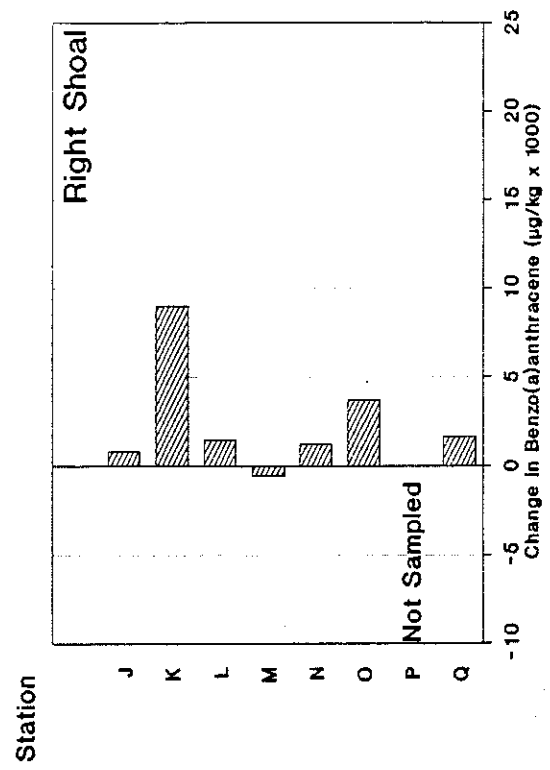
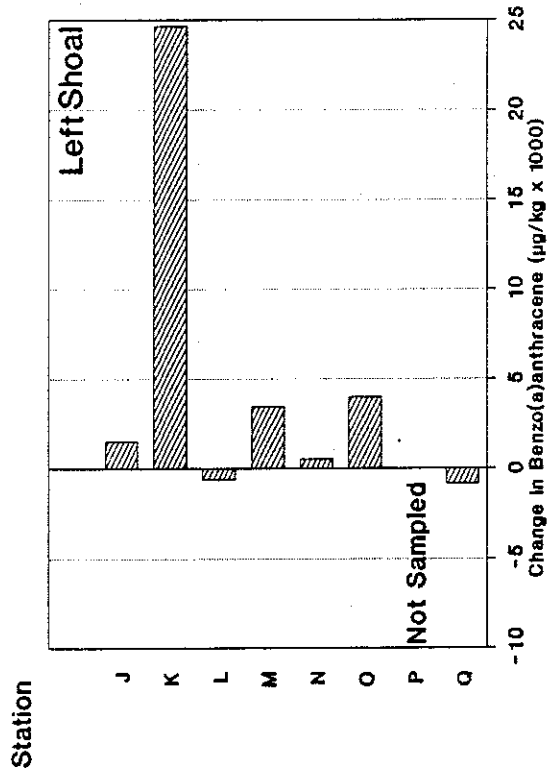
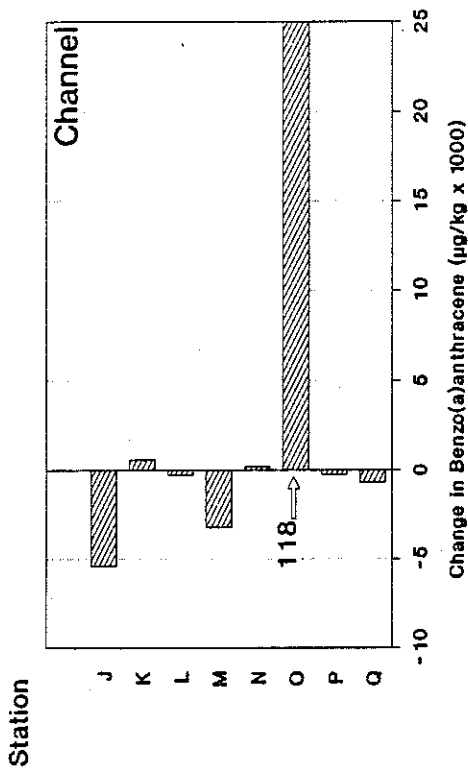
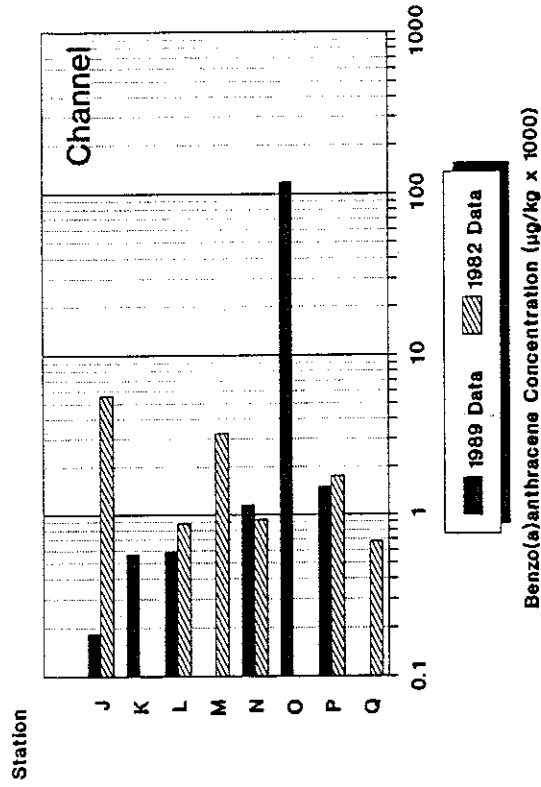
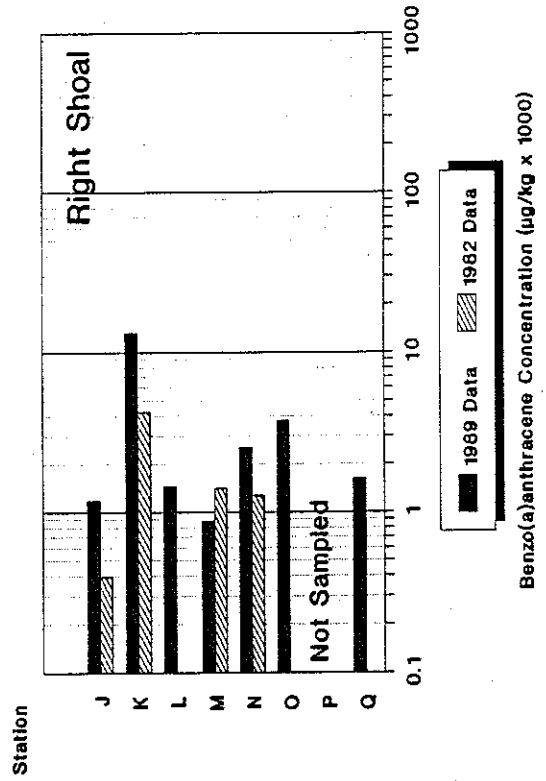
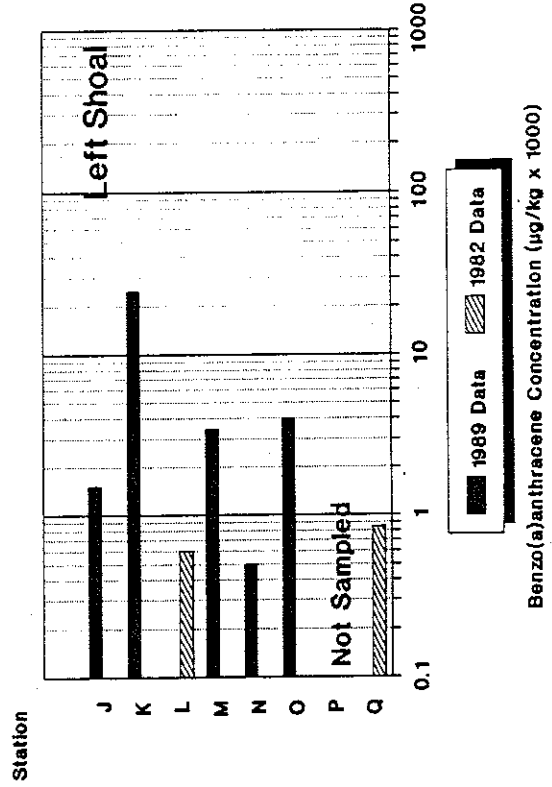


Figure 61. Comparison of benzo(a)anthracene concentrations in Elizabeth River sediments between 1982 and 1989.

Benzo(a)anthracene in Elizabeth River Sediments



Benzo(a)anthracene in Elizabeth River Sediments



1
2
3
4
5
6
7
8
9
10
11
12
13
14
15
16
17
18
19
20
21
22
23
24
25
26
27
28
29
30
31
32
33
34
35
36
37
38
39
40
41
42
43
44
45
46
47
48
49
50
51
52
53
54
55
56
57
58
59
60
61
62
63
64
65
66
67
68
69
70
71
72
73
74
75
76
77
78
79
80
81
82
83
84
85
86
87
88
89
90
91
92
93
94
95
96
97
98
99
100

benzo(a)pyrene (Figs. 62 and 63), benzo(b)fluoranthene (Figs. 64 and 65), chrysene (Figs. 66 and 67), and benzo(ghi)perylene (Figs. 68 and 69). The Site O channel 1989 sample tended to be higher in these heavier PNAs than was the sample from 1979. The depth distributions of the individual PNAs generally confirmed those temporal trends for the low molecular weight and high molecular weight compounds in these regions (see Figures in Appendix D).

The lower molecular weight PNAs tend to be somewhat more soluble and environmentally degradable than the higher molecular weight compounds. The pattern observed for the region in the vicinity of the abandoned creosote factory appears to be decreasing in 2- and 3-ring PNAs, even though the heavier PNAs were in higher concentration in the 1989 samples. This pattern appears to indicate that the contamination is due to a "weathered" creosote source. At the Site K shoals, all of the PNAs increased, indicating "recent" petroleum/combustion sources, possibly associated with shipping, shipyard activities or urban runoff.

In summary, the PNAs in sediments in the Elizabeth River continue to remain in high concentrations in certain regions of the Southern Branch (Sites K-O). The sources of contamination in the upper reaches of this region appear to be associated with creosote, while PNA contamination in the lower reaches appears to be petroleum products from more "active" sources.

Figure 62. Change in benzo(a)pyrene concentrations in Elizabeth River sediments from 1982 to 1989.

CHANGE IN BENZO(a)PYRENE CONCENTRATIONS IN SEDIMENTS FROM 1982 TO 1989

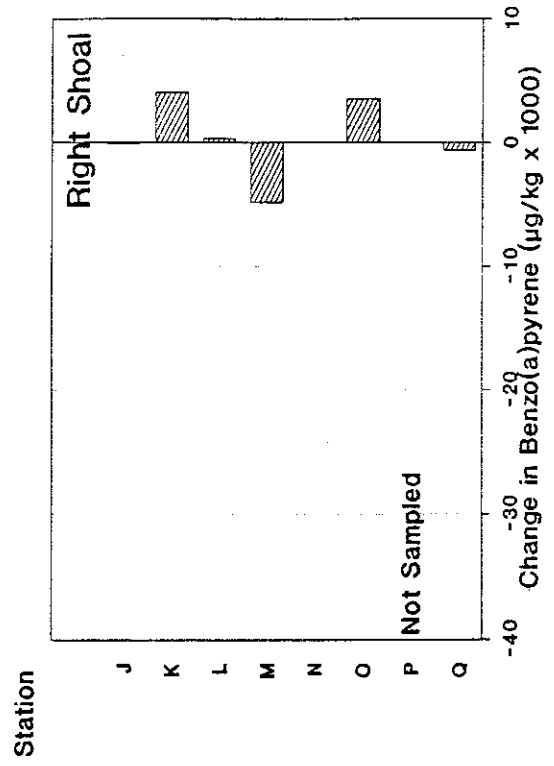
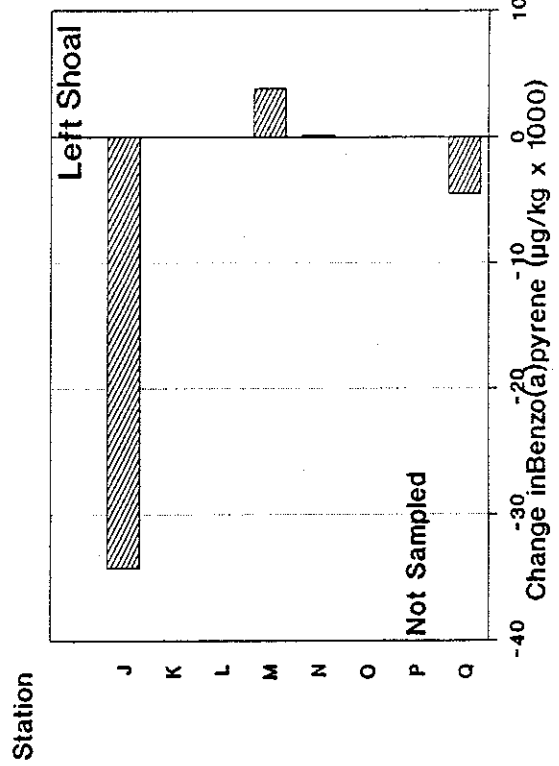
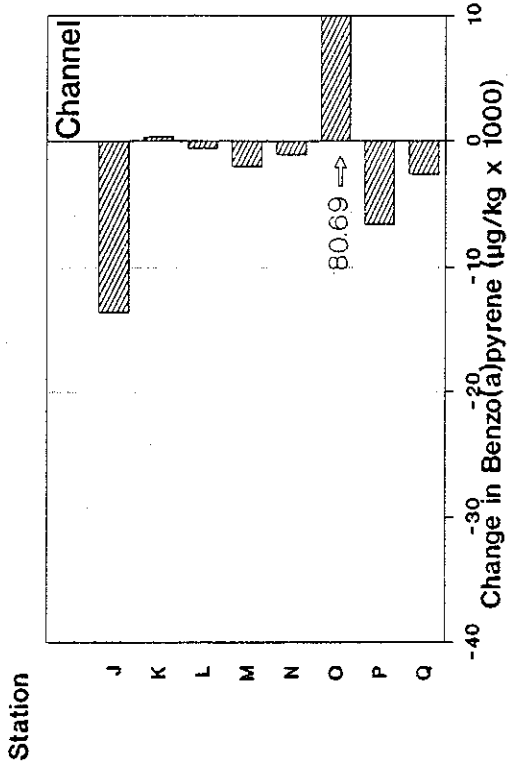
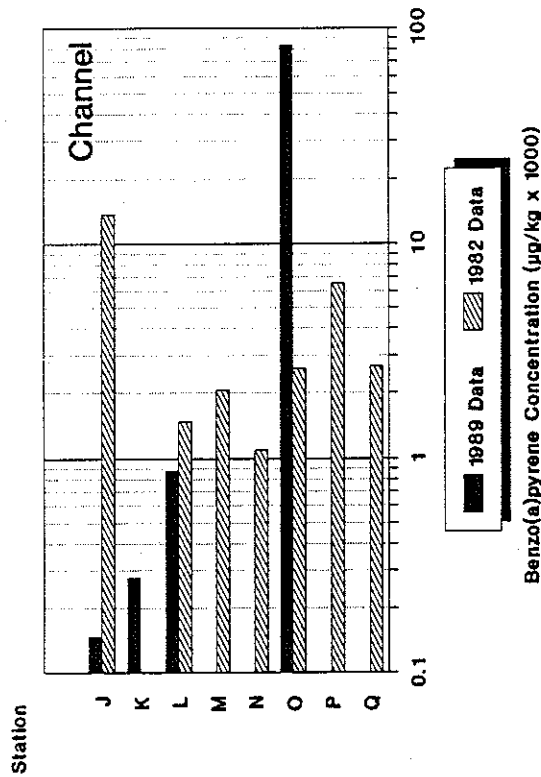
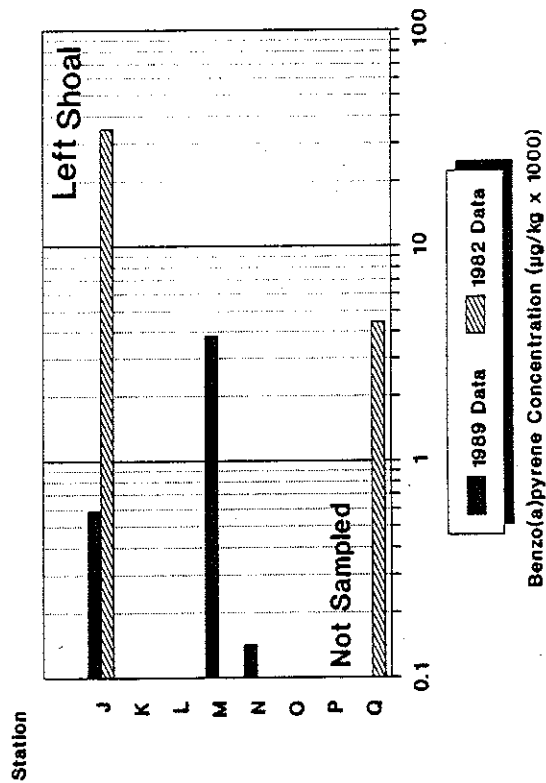


Figure 63. Comparison of benzo(a)pyrene concentrations in Elizabeth River sediments between 1982 and 1989.

Benzo(a)pyrene in Elizabeth River Sediments



Benzo(a)pyrene in Elizabeth River Sediments



Benzo(a)pyrene in Elizabeth River Sediments

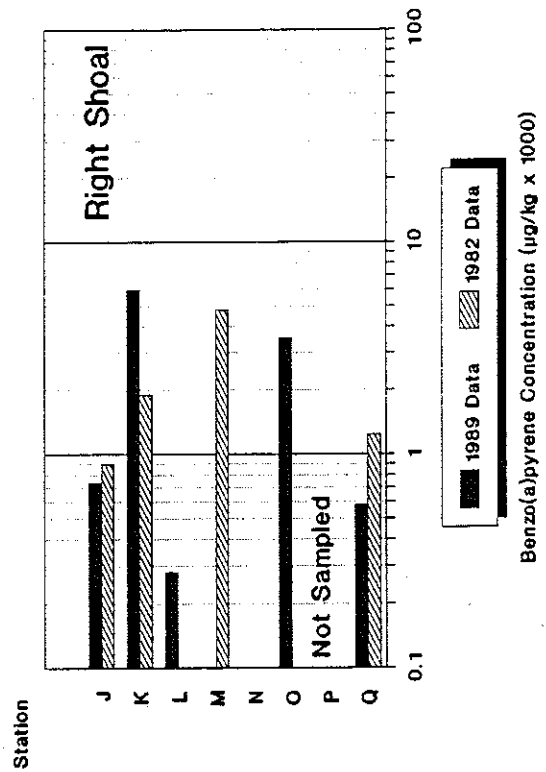


Figure 64. Change in benzo(b)fluoranthene concentrations in Elizabeth River sediments from 1982 to 1989.

CHANGE IN BENZO(b)FLUORANTHENE CONCENTRATIONS IN SEDIMENTS FROM 1982 TO 1989

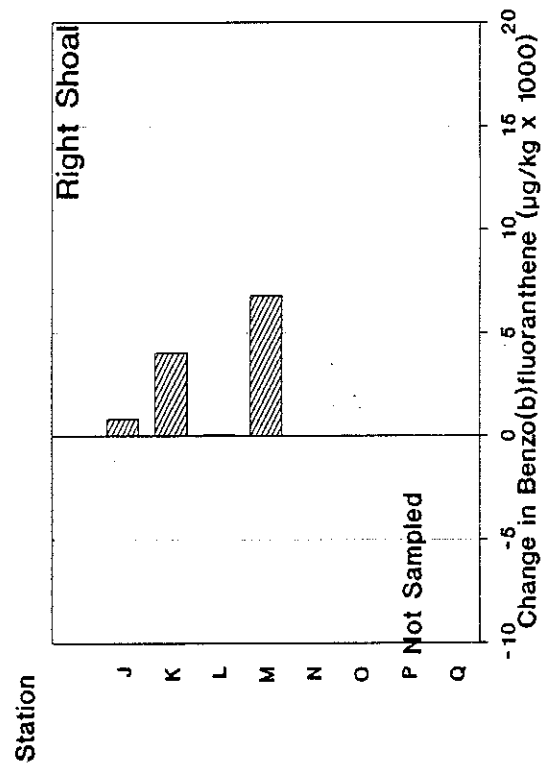
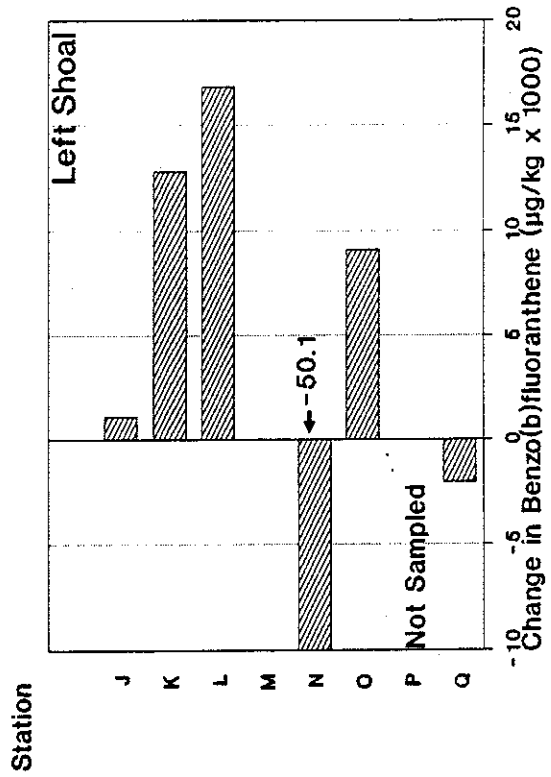
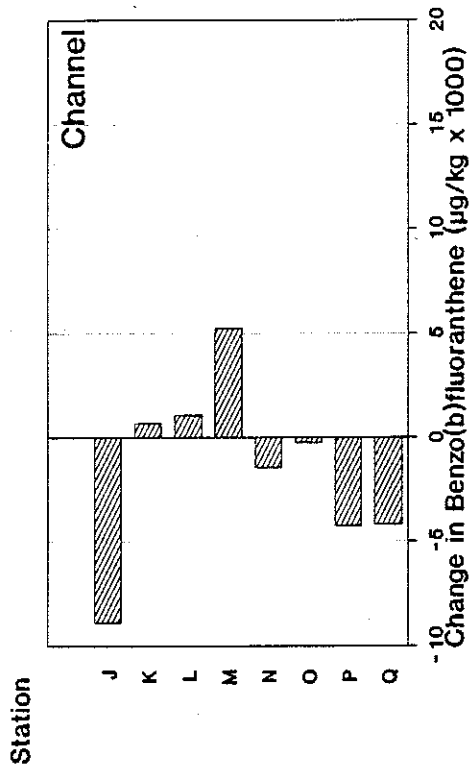
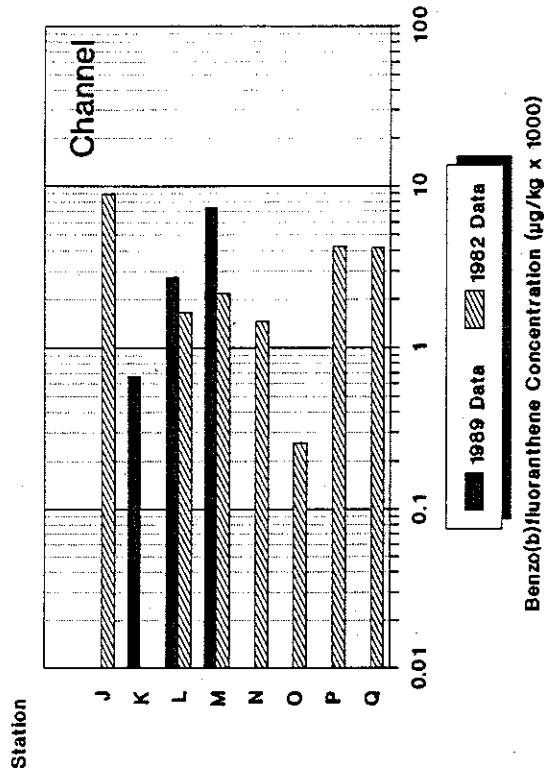


Figure 65. Comparison of benzo(b)fluoranthene concentrations in Elizabeth River sediments between 1982 and 1989.

Benzo(b)fluoranthene in Elizabeth River Sediments



Benzo(b)fluoranthene in Elizabeth River Sediments

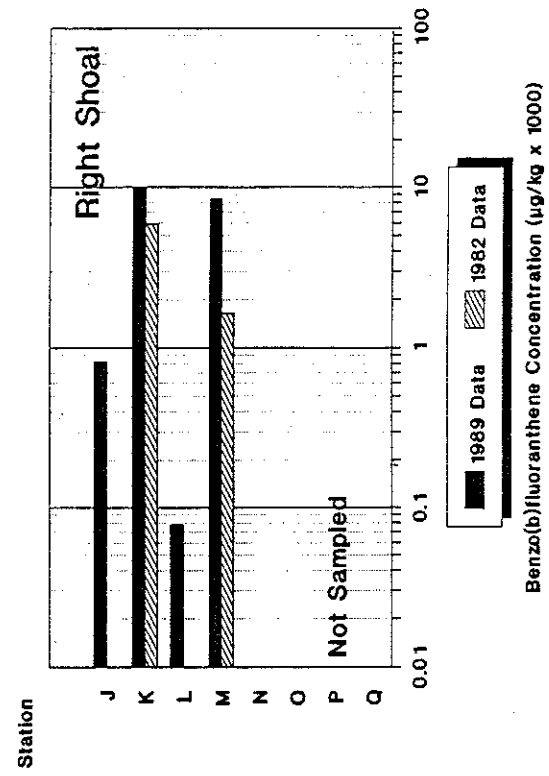
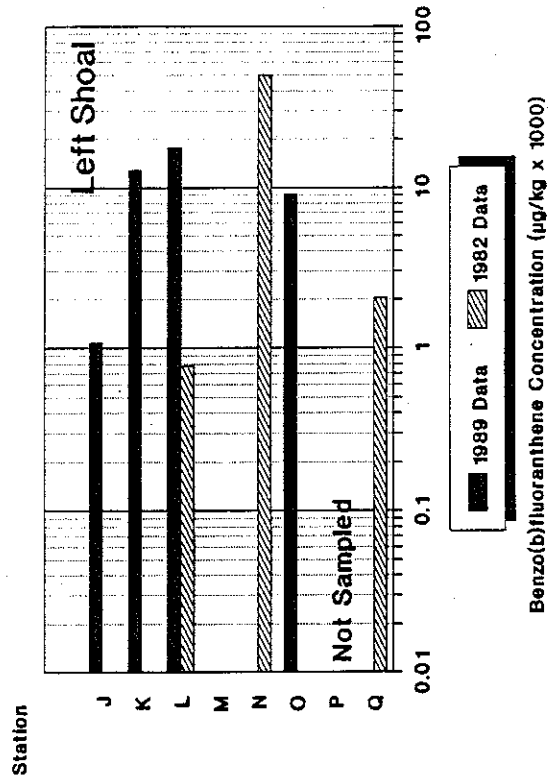


Figure 66. Change in chrysene concentrations in Elizabeth River sediments from 1982 to 1989.

CHANGE IN CHRYSENE CONCENTRATIONS IN SEDIMENTS FROM 1982 TO 1989

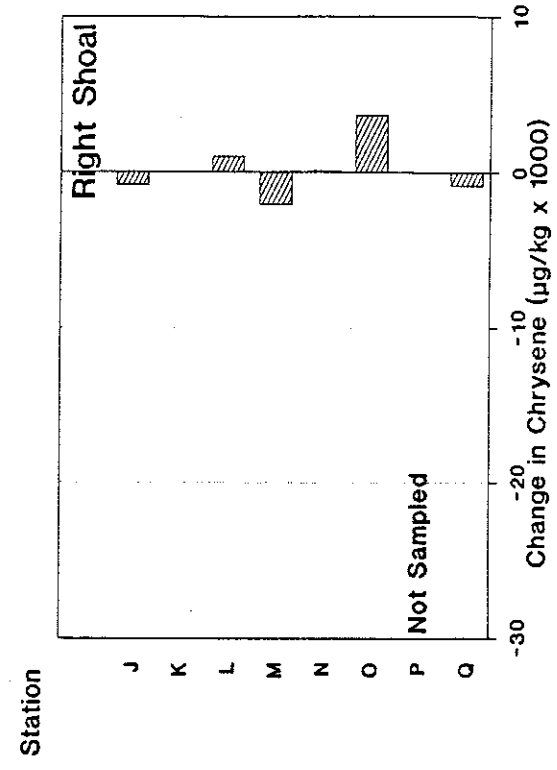
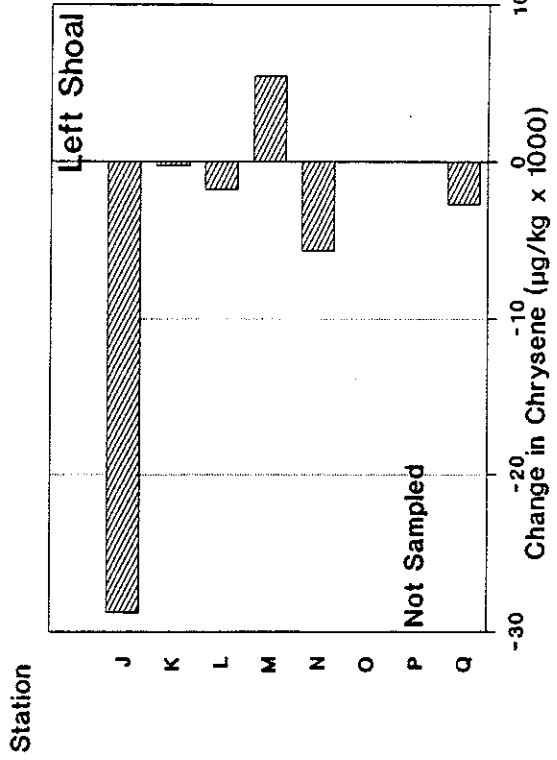
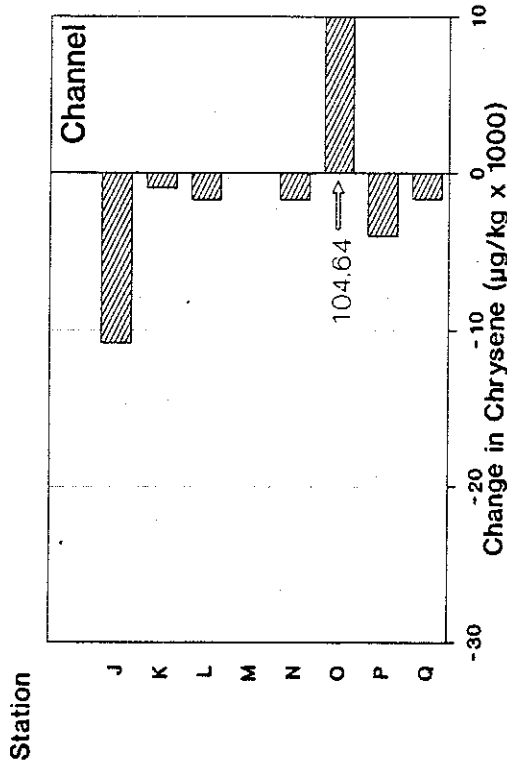
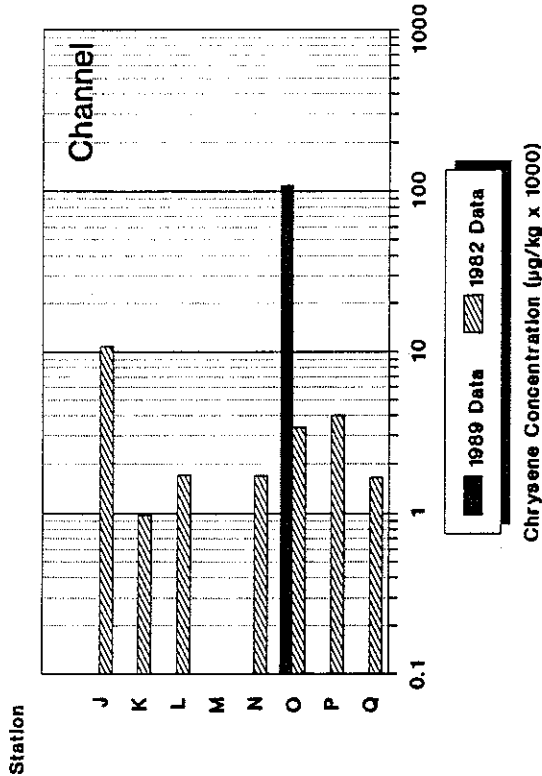
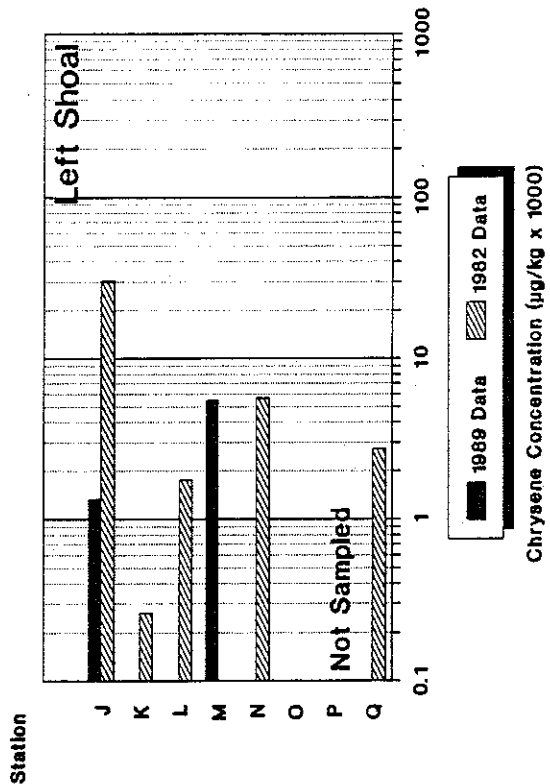


Figure 67. Comparison of chrysene concentrations in Elizabeth River sediments between 1982 and 1989.

Chrysene in Elizabeth River Sediments



Chrysene in Elizabeth River Sediments



Chrysene in Elizabeth River Sediments

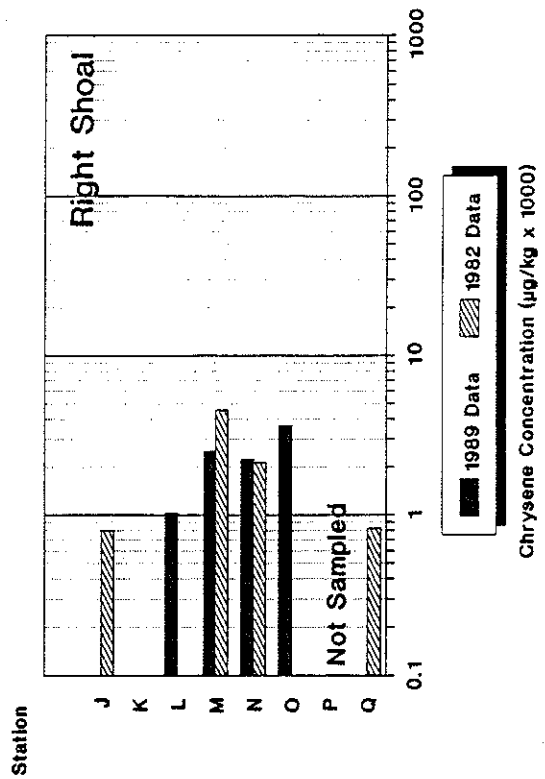


Figure 68. Change in benzo(g,h,i)perylene concentrations in Elizabeth River sediments from 1982 to 1989.

CHANGE IN BENZO(g,h,i)PERYLENE
CONCENTRATIONS
IN SEDIMENTS FROM 1982 TO 1989

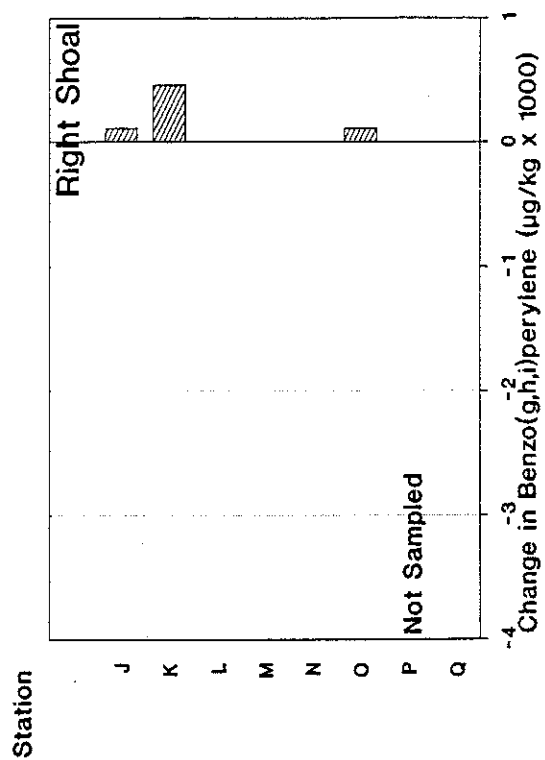
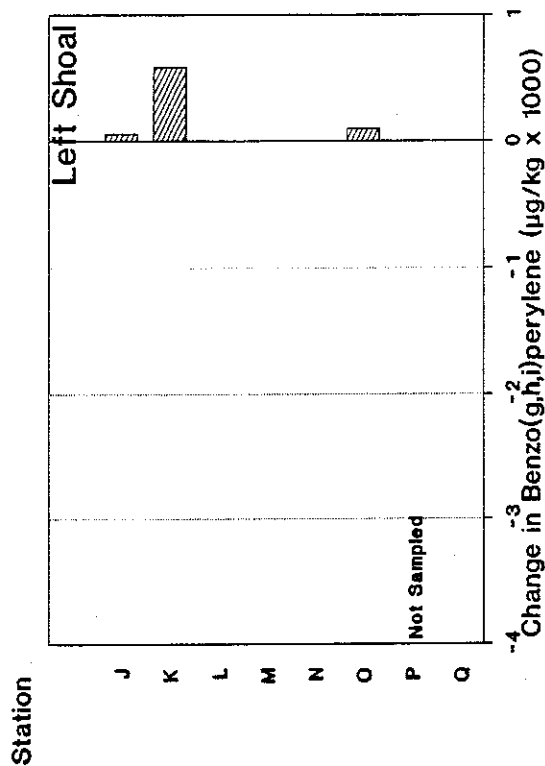
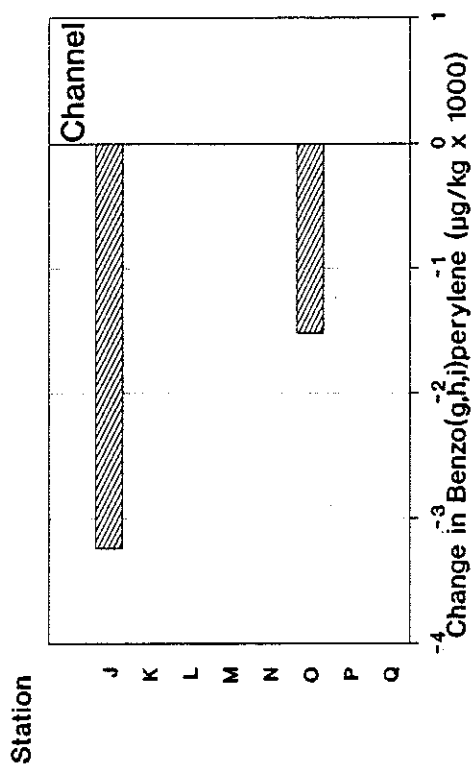
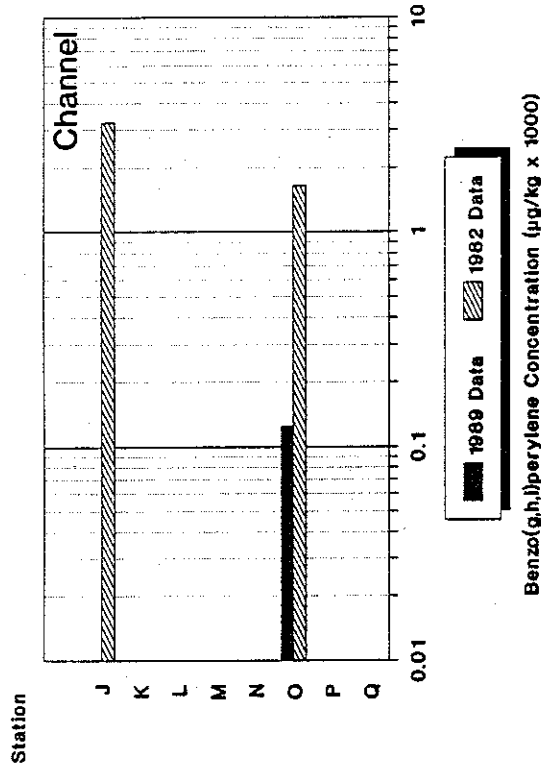
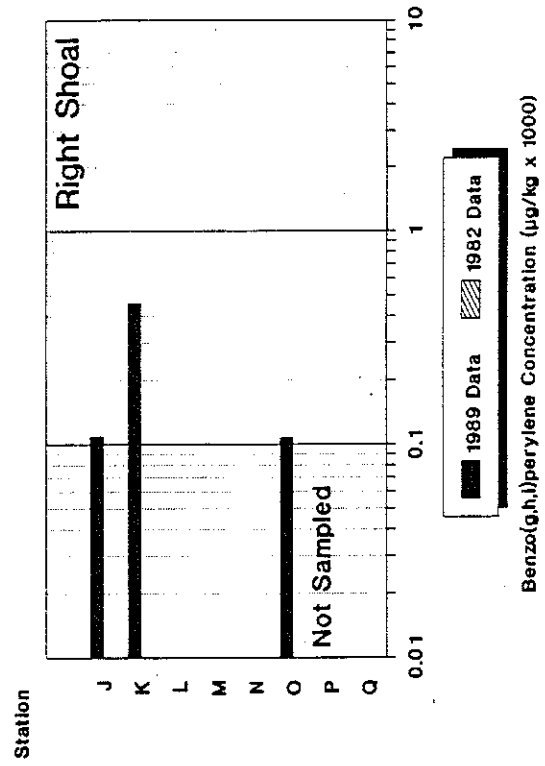
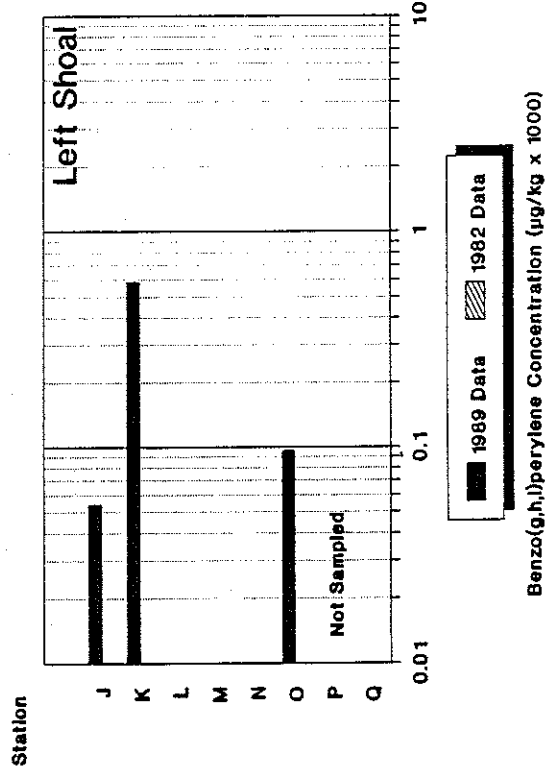


Figure 69. Comparison of benzo(g,h,i)perylene concentrations in Elizabeth River sediments between 1982 and 1989.

Benzo(g,h,i)perylene in Elizabeth River Sediments



Benzo(g,h,i)perylene in Elizabeth River Sediments Benzo(g,h,i)perylene in Elizabeth River Sediments



Benzo(g,h,i)perylene Concentration (µg/kg x 1000)

Benzo(g,h,i)perylene Concentration (µg/kg x 1000)

1
2
3
4
5
6
7
8
9
10
11
12
13
14
15
16
17
18
19
20
21
22
23
24
25
26
27
28
29
30
31
32
33
34
35
36
37
38
39
40
41
42
43
44
45
46
47
48
49
50
51
52
53
54
55
56
57
58
59
60
61
62
63
64
65
66
67
68
69
70
71
72
73
74
75
76
77
78
79
80
81
82
83
84
85
86
87
88
89
90
91
92
93
94
95
96
97
98
99
100

SEDIMENT FLUXES OF ORGANIC CONTAMINANTS

METHODS

Sample Collection and Experimental Procedures

Sediment samples were collected from three sites (EB, J, and M; see Figure 1 and Table 8) on May 15, 1990, utilizing a box corer equipped with a stainless steel liner (16 x 22 x 33 cm). Following deployment of the corer, the entire unit was retrieved and the liner removed. A glass cylindrical core (9 x 33 cm) was driven through the rectangular core contained by the steel liner. A gasket lined plexiglass plate was inserted at the base of the liner, forming a secure seal with the cylindrical core base. The steel liner was then removed and the excess sediment and water were washed from around the inner glass core. A layer of teflon film and a sealing plate were placed on top of the glass core and four threaded polyvinyl chloride (PVC) posts with knurled nuts were installed to secure the two plates to the core sample. The assembled core sample (see Figure 70), containing both the sediment and the overlying water, was immediately placed into a cooler containing bottom water in order to maintain ambient temperatures. Approximate water and sediment volumes of each core are listed in Table 9. Salinity, conductivity, temperature, and dissolved oxygen readings were taken at the time of collection (Table 10).

Table 9. Sediment contaminant flux sampling locations and sediment and water volume data for the samples.

<u>Site</u>	<u>Loran Coordinates</u>	<u>AMRL Sample No.</u>	<u>Sediment Volume (cm³)</u>	<u>Water Volume (cm³)</u>
M	36°48.63'N, 76°16.99'W	34002	1015	490
		34003	775	730
		34004	1185	320
EB	36°50.25'N, 76°15.96'W	34005	905	600
		34006	1165	340
J	36°50.94'N, 76°17.39'W	34008	815	690
		34009	1055	450

Table 10. Field physicochemical data for the sediment collection sites. Asterisk (*) indicates value not determined.

<u>Site</u>	<u>Depth</u>	<u>Salinity (ppt)</u>	<u>Conductivity (mhos/cm)</u>	<u>Water Temp. (oC)</u>	<u>DO (mg/l)</u>
EB	Surface	18.3	29.7	19.9	5.91
EB	Bottom	19.5	31.4	19.1	5.93
M	Surface	19.4	30.2	18.8	5.79
M	Bottom	21.9	34.9	17.7	4.60
J	Surface	*	*	19.7	6.93
J	Bottom	19.7	31.7	19.1	6.22

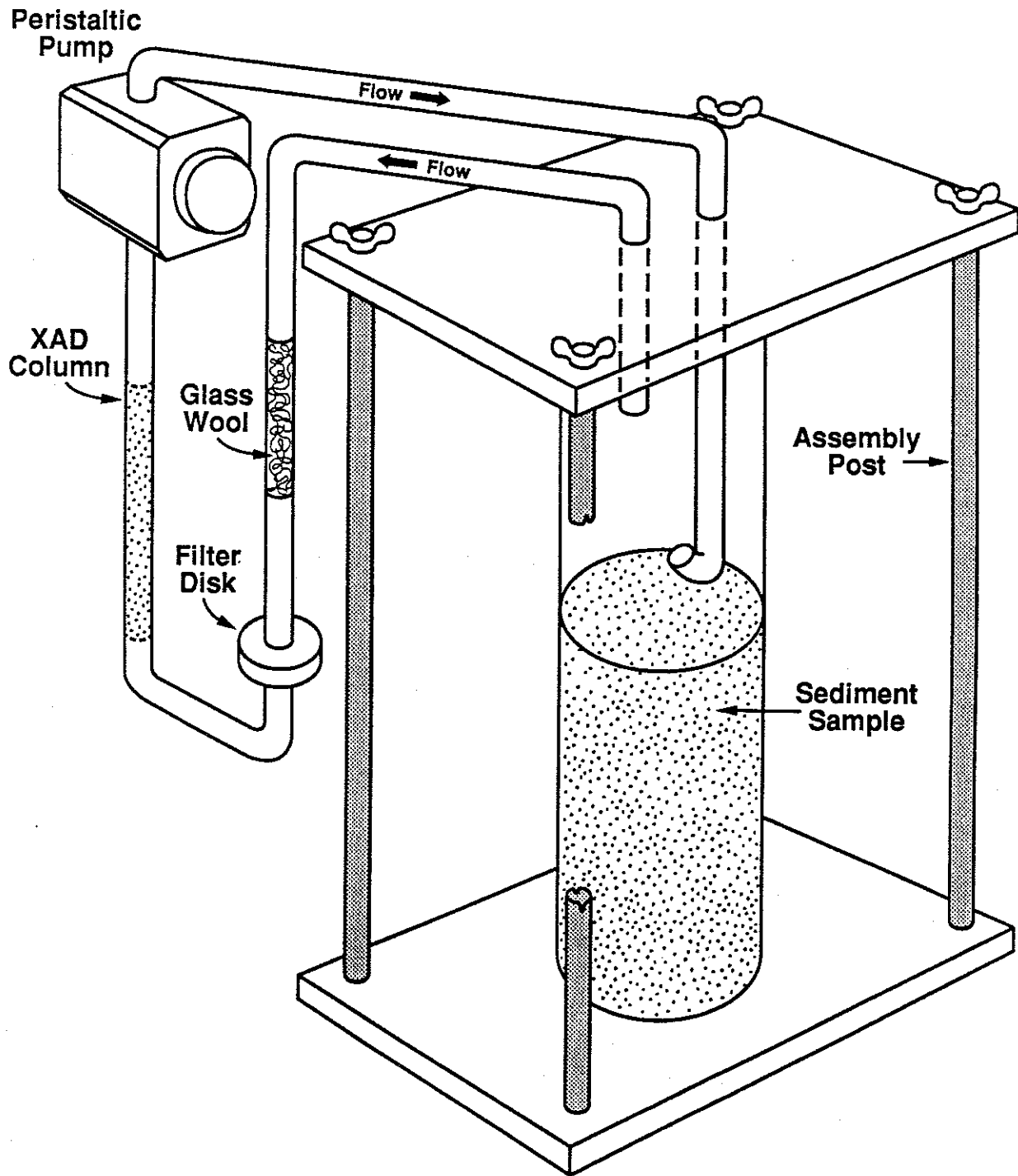


Figure 70. Schematic diagram of the sediment contaminant flux chamber.

Upon return to the laboratory, samples were stored overnight in a chamber equilibrated to a constant temperature similar to that found in the *in situ* bottom waters. All samples were maintained at $19.5 \pm 1^\circ\text{C}$ throughout the duration of the experimental process. Prior to assembly of the flux-flow system, the overlying water of each core was carefully removed and replaced with clean, artificial seawater adjusted to a salinity of 20 ± 1 ppt. Each sample was then placed in-line with the flux-flow system presented in Figure 70. Each flux-flow series contained a glass tube to withdraw water samples from the core, a large particle filter followed by a small particle filter, a column containing 2.5 g (10 cc) of XAD-2 microreticular sorbent resin, and finally a glass inlet tube to re-introduce the sorbent-extracted water back into the core chamber. The water sample was then circulated with a rotary peristaltic pump system. The basic premise of the design was to remove any suspended particulates greater than $0.45 \mu\text{m}$ in diameter and extract the filtered water with the XAD-2 resin column. The water was then reintroduced into the core chamber in such a way that the sediment surface would not be disturbed, and that the re-introduced water would not be withdrawn prior to sufficient contact with the substrate bed surface.

Each flux-flow series was adjusted to operate in such a manner as to circulate 5 ± 0.5 ml of sample water per minute. The system was allowed to proceed at this rate for 24 hours. At the end of the flow period, the two filters were replaced and the adsorbing column was replaced with a new XAD-2 column. The system was

reactivated and allowed to flow for an additional 24 hrs. A basic assumption was made that a relatively constant amount of organics should flux from the sediment phase during the course of the study (48 hrs). Therefore, the two XAD-2 resin columns utilized with each flux chamber act as sequential indications of flux rates. The temperature of the chamber water was monitored every 8 hrs, and any necessary adjustments were made to the cooler bath with hot or cold tap water.

The XAD-2 resin from each adsorbent column was removed and combined with 50 ml of methylene chloride. This mixture was vigorously extracted for 5 minutes, followed by vacuum filtration and collection of the extraction solvent. This process was repeated twice more for each sample column. The pooled extract for each column was concentrated to a final volume and analyzed by gas chromatography/mass spectrometry techniques for the base/neutral/acid compounds listed in Table 11 as well as the 42,000 compounds contained in the National Bureau of Standards (NBS) library. The detection limit for each compound was determined to be approximately 0.2 μ g per adsorbent column.

Following the completion of the flux experiment, the top 2 cm of each sediment core sample was recovered and thoroughly mixed. Subsamples of each 2 cm composite were analyzed for total organic carbon and for some of the organic compounds investigated in the column analyses. Briefly, a 30 g aliquot of each sample was sonication extracted, filtered, and concentrated to a final volume of 1 ml and analyzed in accordance with U.S. E.P.A SW-846 Manual

Table 11. Base/Neutral/Acid extractable organic compounds analyzed for in the sediment flux samples.

<u>CAS No.</u>	<u>Compound</u>
62-53-3	ANILINE
95-57-8	2-CHLOROPHENOL
111-44-4	BIS(2-CHLOROETHYL) ETHER
108-95-2	PHENOL
541-73-1	1,3-DICHLOROPHENOL
106-46-7	1,4-DICHLOROPHENOL
95-50-1	1,2-DICHLOROPHENOL
100-51-6	BENZYL ALCOHOL
39638-32-9	BIS(2-CHLOROISOPROPYL) ETHER
91-57-6	2-METHYLPHENOL
67-72-1	HEXACHLOROETHANE
621-64-7	N-NITROSO-DI-N-PROPYLAMINE
106-44-5	4-METHYLPHENOL
98-95-3	NITROBENZENE
78-59-1	ISOPHORONE
88-75-5	2-NITROPHENOL
65-85-0	BENZOIC ACID
105-67-90	2,4-DIMETHYLPHENOL
111-91-1	BIS(2-CHLOROETHOXY) METHANE
120-83-2	2,4-DICHLOROPHENOL
120-82-1	1,2,4-TRICHLOROBENZENE
91-20-3	NAPHTHALENE
106-47-8	4-CHLOROANILINE
87-68-3	HEXACHLOROBUTADIENE
59-50-7	4-CHLORO-3-METHYLPHENOL
91-57-6	2-METHYLNAPHTHALENE
77-47-4	HEXACHLOROCYCLOPENTADIENE
88-06-2	2,4,6-TRICHLOROPHENOL
95-95-4	2,4,5-TRICHLOROPHENOL
91-58-7	2-CHLORONAPHTHALENE
88-74-4	2-NITROANILINE
208-96-8	ACENAPHTHALENE
84-66-2	DIMETHYLPHTHALATE
606-20-2	2,6-DINITROTOLUENE
99-09-2	3-NITROANILINE
83-32-9	ACENAPHTHENE
51-28-5	2,4-DINITROPHENOL
132-64-5	DIBENZOFURAN
100-02-7	4-NITROPHENOL
121-14-2	2,4-DINITROPHENOL
86-73-7	FLUORENE
7005-72-3	4-CHLOROPHENYL-PHENYLEETHER
84-66-2	DIETHYLPHTHALATE
100-01-6	4-NITROANILINE
534-52-1	4,6-DINITRO-2-METHYLPHENOL
86-30-6	N-NITROSODIPHENYLAMINE
101-55-3	4-BROMOPHENYL-PHENYLEETHER

Table 11 (Cont.)

<u>CAS No.</u>	<u>Compound</u>
118-74-1	HEXACHLOROBENZENE
87-86-5	PENTACHLOROPHENOL
85-01-8	PHENANTHRENE
120-12-7	ANTHRACENE
84-74-7	DI-N-BUTYLPHTHALATE
206-44-0	FLUORANTHENE
129-00-0	PYRENE
85-68-7	BUTYLBENZYLPHTHALATE
56-55-3	BENZO (A) ANTHRACENE
218-01-9	CHRYSENE
91-94-1	3,3-DICHLOROBENZIDINE
117-81-7	BIS (2-ETHYLHEXYL) PHTHALATE
117-84-0	DI-N-OCTYLPHTHALATE
205-99-2	BENZO (B) FLUORANTHENE
207-08-9	BENZO (K) FLUORANTHENE
50-32-8	BENZO (A) PYRENE
193-39-5	INDENO (1,2,3-CD) PYRENE
53-70-3	DIBENZ (A,H) ANTHRACENE
191-24-2	BENZO (G,H,I) PERYLENE
103-33-3	AZOBENZENE
92-87-5	BENZIDINE

Methods 3550 and 8270. Analytical results were determined in $\mu\text{g}/\text{kg}$ dry weight. Percent moisture and specific gravity were determined for each sample (Table 12); these data were used in the calculations of flux rates.

Table 12. Percent moisture and specific gravity data for surficial sediments in flux chambers.

<u>AMRL Sample No.</u>	<u>Site</u>	<u>Percent Moisture (%)</u>	<u>Specific Gravity (g/ml)</u>
34002	M	71.65	1.06
34003	M	73.26	1.19
34004	M	70.22	1.15
34005	EB	63.00	1.10
34006	EB	62.83	1.08
34008	J	63.30	1.09
34009	J	64.97	1.12

Calculation of Flux Rates for Organic Contaminants

The experiments for estimation of flux rates of the organic contaminants were conducted in a manner different from those of the metals and ammonium. This difference was necessitated by the highly hydrophobic nature of these contaminants which produce water concentrations (and changes in water concentrations over time) which are not readily detectable by current technology. Water

sample volumes required in the detection of organic contaminants in ambient waters typically range from 10-50 liters, volumes obviously not available in flux chambers of any reasonable size. Therefore, the experimental design described above was adopted.

The artificial sea water introduced into the flux chambers was clean and it was cycled through the XAD sorbent column to maintain its "uncontaminated" state. A high extraction efficiency by the sorbent was assumed (i.e. high influx from water to sorbent, and low efflux), so the uptake on the sorbent column was assumed to be approximately equal to the contaminant input from the sediment to the water during the experimental period. The assumption of high extraction efficiency of the sorbent columns is supported by the results of previous studies with XAD resin columns which indicate high recoveries of organic contaminants for loadings that were 3-5 orders of magnitude greater than those observed during the present study (Junk et al, 1974; Olufsen, 1980; Ben-Poorat et al., 1986; Alden et al, unpublished data). Therefore, the loading of the sorbent by any given contaminant over the 24 hr experimental period was assumed to approximate the flux out of the sediments.

The flux measurements were calculated both on an areal and on a concentration basis. The areal fluxes were calculated by dividing the load on the sorbent by the surface area of the sediments in the chamber to produce a flux measurement in units of $\mu\text{g}/\text{m}^2/\text{day}$. The concentration based fluxes were calculated by dividing the sorbent loads by the volume of water passing through the columns to produce flux measurements in units of $\mu\text{g}/\text{l}/\text{day}$.

In addition to the calculation of these empirical flux measurements for each contaminant/site combination, more general relationships were sought to produce numerical models which could be applied to other areas within the system and/or similar types of contaminants. A "kinetic" approach similar to that used in bioconcentration experiments (see e.g., Davies and Dobbs, 1984) was employed to estimate rate coefficients for these models. The rate of change equations are as follows:

$$dC_s/dt = k_1C_w - k_2C_s \quad [1]$$

and

$$dC_w/dt = k_2C_s - k_1C_w \quad [2]$$

where the rate of change in the concentration of the sediment (eq. 1) or the water (eq. 2) is a function of the concentration in each component (C_w = concentration in water and C_s = concentration in sediments) and the flux constants k_1 and k_2 . The k_1 constant is the coefficient for movement of the chemical of concern from the water column to the sediment (influx), while k_2 is the coefficient for movement of the chemical from the sediment to the water (efflux). At steady state, the rates of change equal zero, producing the following relationship:

$$\frac{k_1}{k_2} = \frac{C_s}{C_w} = k_{oc} \quad [3]$$

For a large number of nonpolar organic chemicals, investigators have established relationships between the logarithm of this ratio (called the K_{oc} , if the sediment concentrations have been standardized to organic carbon content by dividing by the fractional percent total organic carbon) and the log P (logarithm of the octanol-water partition coefficient) and/or the logarithm of the solubility of the chemical in water (Karickhoff et al., 1979; Karickhoff, 1980; Kenaga and Goring 1980; Brown and Flagg 1981; Rodgers et al., 1984; Pavlou, 1984; Tetra Tech, 1986; and others). This sort of relationship provides a mechanism to estimate the relative magnitude of the flux coefficients since both are a function of the log P or the logarithm of solubility (hereafter referred to as log S) for any given chemical.

In the flux experiments, the water concentration is considered negligible, so the second part of equation 2 drops out to produce:

$$\text{Flux} = dC_w/dt = k_2 C_s \quad [4]$$

or, by rearrangement,

$$\text{Flux}/C_s = k_2 \quad [5]$$

If the relationship between the flux coefficients and log P or log S hold true for the data set from the present study, empirical relationships should exist such that:

$$\log (\text{Flux}/C_s) = \log k_2 = a+b \log P \quad [6]$$

or

$$\log (\text{Flux}/C_s) = \log k_2 = c+d \log S \quad [7]$$

where a, b, c and d are regression coefficients. It should be noted that b should be negative, while d should be positive to reflect the fact that the more hydrophobic (and less soluble) a chemical is, the lower the flux to sediment concentration ratio. Once k_2 has been estimated, k_1 can be derived, if K_{oc} is known for a given chemical. Although a number of empirical equations exist, the following is a commonly used model for predicting K_{oc} from the log P of the chemical:

$$\text{Log } K_{oc} = (0.989 \log P) - 0.346 \quad [8]$$

(Karickhoff, 1981; Pavlou, 1984; Tetra Tech, 1986). Therefore, the k_1 constant can be calculated from equations 3, 6 or 7, and 8:

$$\log k_1 = \log k_{oc} + \log k_2 \quad [9]$$

With the k_1 and k_2 estimates, concentrations in sediment and water, and the log P of a chemical of concern, flux estimates can be calculated from equations 1 and 2 for conditions observed in the River.

RESULTS & DISCUSSION

Flux of Organic Contaminants

The results of the flux experiments are presented in Table 13 and 14. The organic carbon normalized concentrations of PNAs in sediments are presented in Table 15. Flux measurements were calculated for the six PNAs which were observed both in the sediment and in the sorbent. Average fluxes at the three sites ranged from 43 to 1000 $\mu\text{g m}^2\text{day}^{-1}$ or 0.03 to 0.65 $\mu\text{g l}^{-1}\text{day}^{-1}$. It should be noted that these rates could be somewhat biased upward due to the fact that observations for which contaminants were below detection limits in the sorbent extractions were not included in the calculations (i.e. treated as missing) rather than setting the fluxes to zero. As with most issues related to censored data (i.e. data with values that are below detection limits), each of these options represents a subjective decision which may bias the calculations in an upward or downward manner. However, it was decided that the upward bias was preferable as the "environmentally conservative" option.

The concentrations of PNAs in the sediment (Table 15) were within the range of concentrations observed for the cores described in earlier sections of this report (**Organic Contaminants: Overall Spatial Patterns and Organics Data by Site**), except that one of the cores from site J had high levels of benzo(b)fluoranthene, which produced a measurable flux in one of the tests.

Table 13.

Flux of organic contaminants from Elizabeth River sediments ($\mu\text{g}/\text{m}^2/\text{day}$). Calculations of mean fluxes and standard errors were based upon sample/ observations combinations for which detectable concentrations were observed. The "Average" row presents averages of all samples for which a flux could be calculated.

<u>Site</u>	<u>Naphthalene</u>	<u>Methylnaphthalene</u>	<u>Phenanthrene</u>
EB	419 \pm 312	505 \pm 118	172*
J	597 \pm 260	1000 \pm 204	172*
M	233 \pm 33	43*	258 \pm 92
Average	385 \pm 102	611 \pm 195	229 \pm 62

<u>Site</u>	<u>Pyrene</u>	<u>Fluoranthene</u>	<u>Benzo(b) Fluoranthene</u>
EB	258 \pm 151	258 \pm 129	-
J	122 \pm 19	143 \pm 19	86*
M	-	151 \pm 22	-
Average	176 \pm 59	178 \pm 36	86*

Table 14. Change in concentrations of water exposed to Elizabeth River sediments ($\mu\text{g}/\text{l}/\text{day}$).

<u>Site</u>	<u>Naphthalene</u>	<u>Methylnaphthalene</u>	<u>Phenanthrene</u>
EB	0.27 \pm 0.20	0.33 \pm 0.08	0.11*
J	0.38 \pm 0.17	0.65 \pm 0.13	0.11*
M	0.15 \pm 0.02*	0.03*	0.17 \pm 0.06
Average	0.25 \pm 0.07	0.39 \pm 0.13	0.15 \pm 0.04

<u>Site</u>	<u>Pyrene</u>	<u>Fluoranthene</u>	<u>Benzo(b) Fluoranthene</u>
EB	0.17 \pm 0.10	0.17 \pm 0.08	-
J	0.08 \pm 0.01	0.09 \pm 0.01	0.06*
M	-	0.10 \pm 0.01	-
Average	0.11 \pm 0.04	0.12 \pm 0.02	0.06*

* Observed in only one of the sample/observation period combinations.

Table 15. Concentration of PNAs in sediments of the Elizabeth River normalized to organic carbon ($\mu\text{g}/\text{kg}$ o.c.).

<u>Site</u>	<u>Naphthalene</u>	<u>Methylnaphthalene</u>	<u>Phenanthrene</u>
EB	1399 \pm 325	868 \pm 128	11743 \pm 3263
J	2392 \pm 419	1884 \pm 11	38280 \pm 7149
M	548 \pm 41	813 \pm 77	5854 \pm 685
Average	1318 \pm 253	1218 \pm 164	16801 \pm 4336

<u>Site</u>	<u>Pyrene</u>	<u>Fluoranthene</u>	<u>Benzo(b) Fluoranthene</u>
EB	18360 \pm 2995	25419 \pm 5182	-
J	42680 \pm 5334	68722 \pm 16567	471073*
M	18533 \pm 1478	27278 \pm 7217	32937
Average	25383 \pm 3469	38588 \pm 7512	178158 \pm 92629

* Observed in only one of the sample/observation period combinations.

The relationship between the flux to concentration ratio and the log P of the contaminants is presented in Figure 71, while the relationship to log S is presented in Figure 72. Both of these relationships were very highly significant ($p < 0.001$) and produced comparable R^2 values ($R^2 = 0.76$ and $R^2 = 0.80$, respectively). The empirical regression equations that fit equations 6 and 7 were as follows:

$$\log (\text{Flux}/C_s) = \log k_2 = 0.397 + (-1.181 \log P)$$

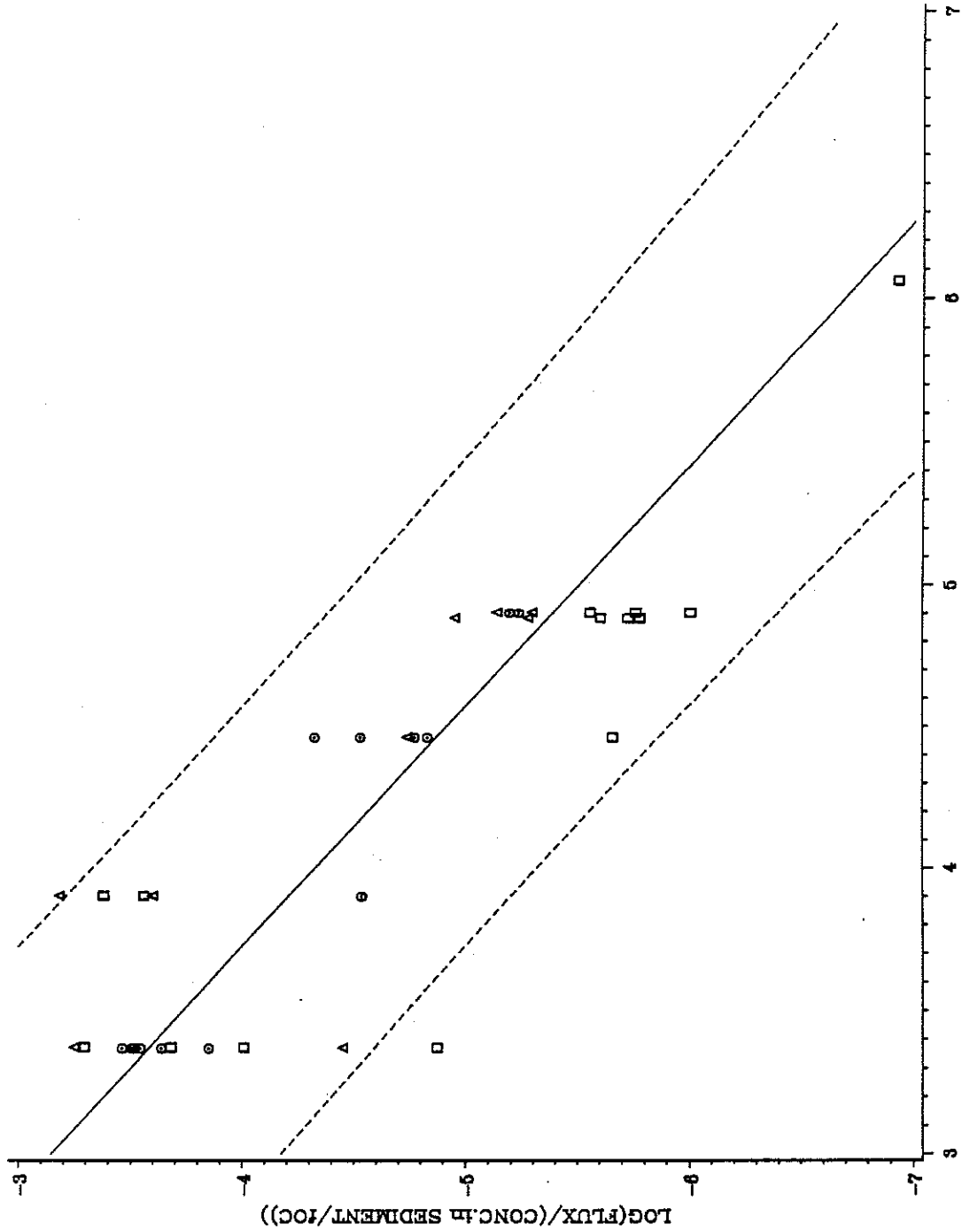
and

$$\log (\text{Flux}/C_s) = \log k_2 = -4.908 + (0.809 \log S).$$

The value for the k_1 coefficient could be calculated for a chemical with a given log P by the k_2 estimates and equations 8 and 9. Rough estimates of flux rates for similar contaminants could be made by utilizing ambient concentrations, the k_1 and k_2 values and equations 1 and 2. However, it should be emphasized that these relationships are extremely preliminary in nature, since they are based upon relatively few samples. Furthermore, the K_{oc} equations were derived for a fairly dilute mixture of sediments suspended in water (Karickhoff, 1981), which may not reflect the dynamics of diffusion across the sediment/water boundary layer and/or may not fit the higher sediment-water ratio involved in in situ partitioning (Tetra Tech, 1976). Therefore, future validation and refinement studies will be required before these relationships can be used for more than just "rough cut" estimates of the magnitude of fluxes.

Figure 71. Logarithm of the ratios of sediment flux rates to sediment concentrations versus the log P of organic contaminants.

LOG(FLUX per OC NORMALIZED SEDIMENT CONCENTRATION) versus
LOG P OF ORGANIC CONTAMINANTS



LEGEND □ □ □ STATION J △ △ △ STATION EB ○ ○ ○ STATION M ——— R-SQ. = 0.76

Figure 72. Logarithm of the ratios of sediment flux rates to sediment concentrations versus the logarithm of the solubilities ($\log S$) of organic contaminants.

LOG(FLOW per OC NORMALIZED SEDIMENT CONCENTRATION) versus
LOG SOLUBILITY OF ORGANIC CONTAMINANTS

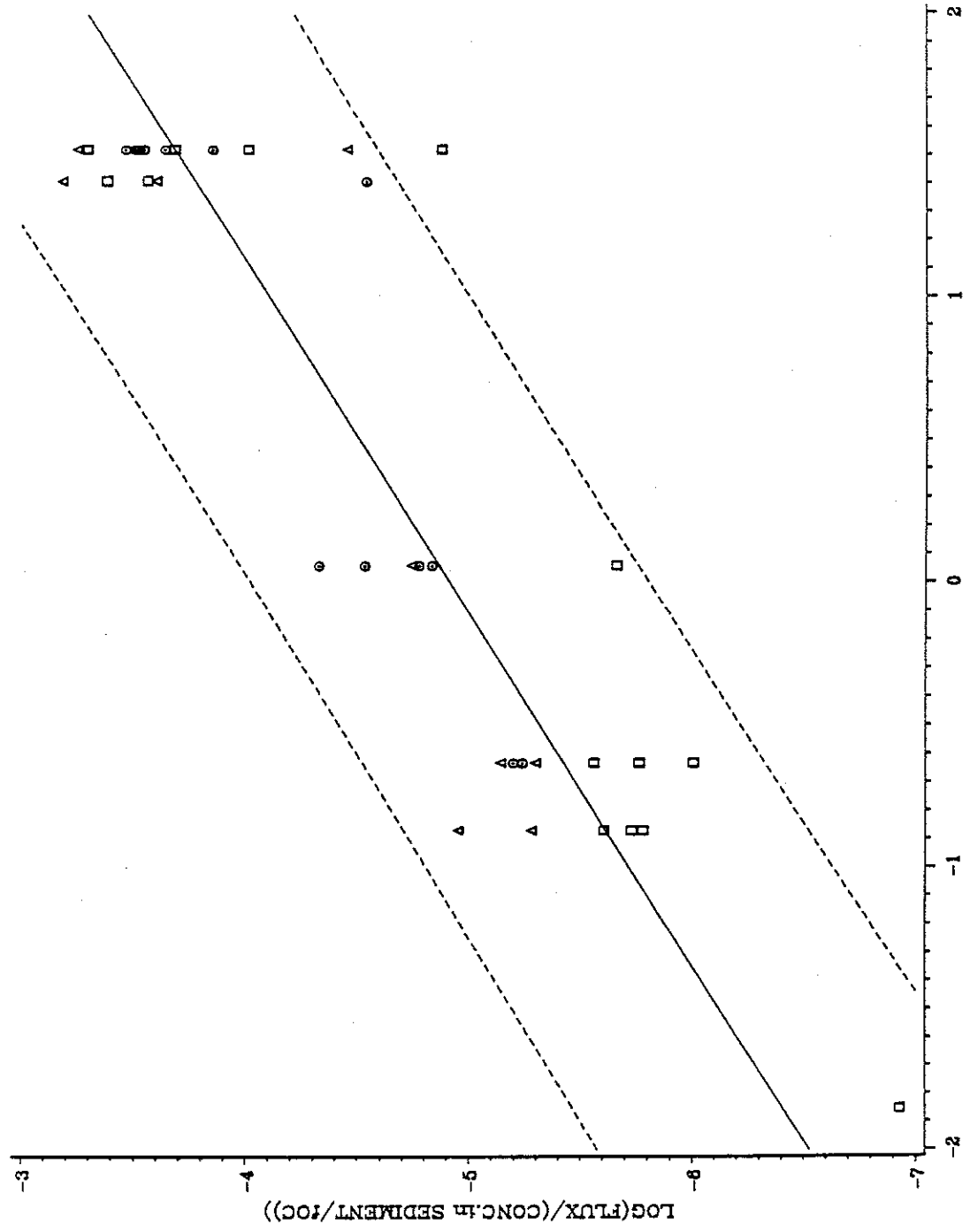


Table 16 presents the flux equation coefficients k_1 and k_2 which were calculated on a concentration and an areal basis. Few, if any, direct estimates of in situ flux coefficients of organic contaminants are available in the literature for comparison purposes. Most of the work on sediment sorption/desorption process has involved either batch experiments of suspended solids in water or flow-through measurements of water passing through a column of sediments (Podoll and Mabey, 1984). In both of these types of experiments, the water and sediment phases are in intimate contact, so that the large surface area presented by the sediment particles is available for sorption processes. On the other hand, in the present study, the sediment-water interface presented a relatively limited surface area for sorption/diffusion processes. Therefore, the flux coefficients for the present study, with an experimental design which represents more closely the in situ conditions at the sediment-water interface of the River, would be expected to be lower than those observed in previous batch or flow-through studies.

For example, k_2 values estimated for the present study (based upon concentrations) were approximately 5 orders of magnitude lower to those reported by Karickhoff (1980) for purge desorption experiments involving suspended solids ($k_2 = 12-23 \text{ day}^{-1}$ for naphthalene; $k_2 = 3.4 \text{ day}^{-1}$ for phenanthrene; and $k_2 = 0.7 \text{ day}^{-1}$ for pyrene). The restriction of the area of close sediment-water contact to the interface surface area clearly limits the desorption rates when compared to those measured when the surface area of all

Table 16.

Flux equation coefficients calculated on a concentration and areal basis for contaminants in the Elizabeth River.

<u>Compound</u>	<u>log P</u>	<u>Concentration Based Coefficients</u>	
		k_1 (day ⁻¹)	k_2 (day ⁻¹)
Napthalene	3.37	2.5×10^{-1}	2.6×10^{-4}
Methylnaphthalene	3.90	2.0×10^{-1}	6.2×10^{-5}
Phenanthrene	4.46	1.6×10^{-1}	1.3×10^{-5}
Pyrene	4.88	1.3×10^{-1}	4.3×10^{-6}
Fluoranthene	4.90	1.3×10^{-1}	4.1×10^{-6}
Benzo(b) Fluoranthene	6.06	7.7×10^{-2}	1.7×10^{-7}
By log P	10 (log K _{oc} + log k ₂)	10 (0.397 - 1.18 log P)	
By log S	10 (log K _{oc} + log k ₂)	10 (-4.91 + 0.809 log S)	

<u>Compound</u>	<u>log P</u>	<u>Aeral Based Coefficients</u>	
		k_1 (day ⁻¹)	k_2 (day ⁻¹)
Napthalene	3.37	59.8	6.2×10^{-2}
Methylnaphthalene	3.90	45.76	1.4×10^{-2}
Phenanthrene	4.46	34.3	2.9×10^{-3}
Pyrene	4.88	27.7	9.2×10^{-4}
Fluoranthene	4.90	27.5	8.7×10^{-4}
Benzo(b) Fluoranthene	6.06	15.2	3.4×10^{-5}
General Equations	All		
By log P	10 (log K _{oc} + log k ₂)	10 (2.866 - 1.210 log P)	
By log S	10 (log K _{oc} + log k ₂)	10 (-2.567 + 0.828 log S)	

suspended particles are involved. Diffusion rates within the sediments may also play a significant role in limiting these rates.

The areal-based rate coefficients (Table 16) are perhaps of greater management use since they would allow "rough cut" estimates of "loadings" from the sediments to the water column. These values were calculated in a manner similar to those for concentration based coefficients except that absolute loads per unit area were considered instead of concentrations: the loading to the water was the mass of contaminants passing across the interface (into the sorbent) per unit area; while the areal sediment contaminant loads were the amount of contaminants per unit area which were collected to a depth of 2 cm (as an assumed limit for sediment diffusion processes, as well as a practical limit that could be collected and analyzed routinely as a segregated layer). Under these defined conditions, the left sides of equations 6 and 7 can be converted to their areal equivalents by multiplying the flux to sediment ratio by the water to sediment mass ratio (i.e. multiply the numerators by the volume of water passing through the chambers and the denominators by estimates of the dry weight of sediments in the top 2 cm layer of sediments in the chamber) to produce units representing the mass of contaminants fluxing into the water per unit area per day normalized (divided by) to the mass of contaminants in the surficial sediments per unit area. The flux coefficients calculated from the data are also higher by factors proportionate to the water to sediment mass ratios of the flux chambers.

The empirical equations (Table 16) relating the flux coefficients to log P values, and surficial sediment contaminant load data can be used to roughly project loading rates for organic contaminants in the River:

$$\text{Flux (area)} = k_{2(\text{area})}C_{s(\text{area})} - k_{1(\text{area})}C_{w(\text{area})} \quad [10]$$

where equation 2 is modified for areal calculations: Flux_(area) is in units of $\mu\text{g m}^{-2} \text{ day}^{-1}$; $k_{1(\text{area})}$, $k_{2(\text{area})}$ are the coefficients derived on areal basis (Table 16); $C_{s(\text{area})}$ is the surficial (2 cm deep) sediment load in units of $\mu\text{g m}^{-2}$ (organic carbon normalized); and $C_{w(\text{area})}$ is the load of the contaminant already in the water column (if it can be detected), also in units of $\mu\text{g m}^{-2}$. For example, if $C_{s(\text{area})} = 8500 \mu\text{g naphthalene m}^{-2}$ (i.e. the average concentration of naphthalene for surficial sediments shown in Table 15 times the projected mass of these sediments per m^2) and the $C_{w(\text{area})} = 1000 \mu\text{g m}^{-2}$ (i.e. $0.2 \mu\text{g/l} = 200 \mu\text{g m}^{-3}$, a concentration occasionally observed in the Elizabeth River, times an assumed water column height of 5 m), equation 10 would become:

$$\begin{aligned} \text{Flux}_{(\text{area})} &= (0.062 \text{ day}^{-1} \times 8,500 \mu\text{g m}^{-2}) - (59.76 \text{ day}^{-1} \\ &\quad \times 1,000 \mu\text{g m}^{-2}) = -59,233 \mu\text{g m}^{-2} \quad [10a] \end{aligned}$$

Thus, the flux would be into the sediments. On the other hand, if the water was "clean" (i.e. naphthalene not detectable), the flux out would only be $527 \mu\text{g m}^{-2} \text{ day}^{-1}$. Considering that the water quality criteria for naphthalene is $620 \mu\text{g/l}$, these levels could never be caused solely by the estimated fluxes from sediments with

the contamination levels observed at these three sites. Another example would be for fluoranthene, a contaminant with a higher log P and greater sediment contaminant concentrations. In this example $C_{s(\text{area})} = 40,000 \mu\text{g m}^{-2}$ (organic carbon normalized) and $C_{w(\text{area})} = 500 \mu\text{g m}^{-2}$ (i.e. the detection limit for 15 l. samples = $0.1 \mu\text{g/l} = 100 \mu\text{g m}^{-3} \times 5\text{m} = 500 \mu\text{g m}^{-2}$) so equation 10 becomes:

$$\text{Flux}_{(\text{area})} = (8.7 \times 10^{-4} \text{ day}^{-1} \times 40,000 \mu\text{g m}^{-2}) - 27.46 \text{ day}^{-1} \times 500 \mu\text{g m}^{-2} = -13,697 \mu\text{g m}^{-2} \quad [10b]$$

or, if clean water were assumed:

$$\text{Flux}_{(\text{area})} = 8.7 \times 10^{-4} \text{ day}^{-1} \times 40,000 \mu\text{g m}^{-2} = 35 \mu\text{g m}^{-2}.$$

The U.S. E.P.A Gold Book chronic water quality criteria for fluoranthene is $16 \mu\text{g/l}$, so this example also indicates that water quality criteria are not likely to be violated due to sediment flux alone. However, the process of flux estimation should prove useful in determining the relative magnitude of contribution of sediment flux processes to the total loading of a chemical to a water body segment.

The closeness of fit of the calculated flux rates to the measured values was determined for all contaminant-sample combinations with a paired t-test. The t-test indicated no significant differences between observed and calculated values for concentration-based fluxes ($p=0.95$) or areal-based fluxes ($p=0.69$). Examination of residuals indicated no significant deviations from normality. The standard errors for differences between observed

and calculated were $0.05 \mu\text{g l}^{-1} \text{ day}^{-1}$ and $78 \mu\text{g m}^{-2} \text{ day}^{-1}$ for concentration and areal flux rates which had mean flux rates of $0.20 \mu\text{g l}^{-1} \text{ day}^{-1}$ and $78 \mu\text{g m}^{-2} \text{ day}^{-1}$, respectively. Corresponding percent error rates (i.e. $[(t \times \text{standard error})/\text{mean}] \times 100$) were $\pm 48\%$ and $\pm 51\%$, based upon the means for concentration-based and flux-based rates, respectively. Thus it appears that, on the average, the calculated rate was within approximately 50% of the observed rate. It should be emphasized that this sort of "confirmation" process does not truly "validate" the flux equations since the same data used to derive the empirical models were used to determine how well they worked. In order to validate the models and to assess how well they generally fit in situ conditions, they should be tested as a priori relationships for other contaminants, in other sediment types, and from other sites within the River. The relatively high degree of fit (R^2 of approximately 0.8) observed for the equations 6 and 7, as well as the relatively small percent errors on the calculated values do suggest that these models may be promising tools for evaluating the relative magnitude of sediment fluxes of nonpolar organic contaminants in loading budgets.

One final set of calculations was performed to provide "worst case" estimates of possible contributions of contaminants to the water column. The relationship presented in equation 3 was rearranged to predict water concentrations of PNAs at equilibrium to the sediments at each site:

$$C_w = \frac{C_s}{K_{oc}}$$

[11]

These estimates are presented in Table 17. Even with these extremely conservative estimates (which were based upon K_{oc} relationships established for sediments suspended in water; see above), the water quality criteria for naphthalene and fluoranthene would not be exceeded due to fluxes from the sediments at these sites.

Despite the interesting potential of the empirical flux models, several caveats (in addition to points already made concerning the preliminary nature of the models and the need for validation with independent data sets) must be made concerning the interpretation of these relationships. First of all, all flux measurements and water quality comparisons are based upon the dissolved organic contaminants. No statements can be made or conclusions drawn concerning the total concentrations or effects of contaminants associated with suspended solids in the River. The suspended solids elutriates created from sediments collected from some of the regions of the Elizabeth River have previously been shown to be quite toxic (Alden and Young, 1982; Alden et al., 1984; Hargis et al., 1984; Alden and Butt, 1988). Suspended solid concentrations in the River may be expected to be quite high during certain conditions, such as those associated with: heavy shipping activities, with large vessels stirring up channel and near-channel sediments; many dredging activities, particularly those involving

Table 17. Estimated concentrations of PNAs in water at equilibrium with sediments ($\mu\text{g/l}$).

<u>Site</u>	<u>Naphthalene</u>	<u>Methylnaphthalene</u>	<u>Phenanthrene</u>
EB	1.44 \pm 0.33	0.27 \pm 0.05	1.01 \pm 0.28
J	2.46 \pm 0.43	0.58 \pm 0.003	3.30 \pm 0.62
M	0.56 \pm 0.04	0.25 \pm 0.02	0.50 \pm 0.06
Average	1.36 \pm 0.26	0.38 \pm 0.05	1.45 \pm 0.37

<u>Site</u>	<u>Pyrene</u>	<u>Fluoranthene</u>	<u>Benzo(b) Fluoranthene</u>
EB	0.61 \pm 0.10	0.80 \pm 0.16	0.07*
J	1.41 \pm 0.18	2.20 \pm 0.52	1.60*
M	0.61 \pm 0.05	0.86 \pm 0.23	0.07*
Average	0.84 \pm 0.11	1.22 \pm 0.24	0.40 \pm 0.21

* Observed in only one of the sample/observation period combinations.

mechanical dredges with hopper barges practicing "economic loading" (i.e. allowing supernatants to overflow until the solids content is high enough to warrant transport); construction activities involving the placement of subtidal or intertidal structures; and storm events. Such conditions, as well as the natural and man-made hydrographic patterns in the River, will be primarily responsible for the transport of particle reactive contaminants such as PNAs, other nonpolar organic contaminants, and most metals in the River (see Appendix A for more discussion). Dynamics, fate, and effects of particle reactive pollutants in the River are poorly understood and should be studied further before management decisions related to activities that may result in large-scale resuspension events may be made effectively.

A second caveat that must be stated concerning the flux models involves points discussed previously concerning the limitations of the Equilibrium Partitioning approach to the development of sediment quality criteria (see section entitled **Assessment of Sediment Quality**). Many of the assumptions implicit in the flux models are based upon K_{oc} equations and other relationships that have not been thoroughly validated for these purposes. The observation that sediment quality criteria derived by the EP approach would not be violated by any sediments yet sampled in the Elizabeth River, and the observation that water quality criteria would not be expected to be violated by any of the flux calculations represent two sides of the same coin. The concerns expressed for the EP approach should be echoed at this point. In

particular, it should be emphasized that interactions between contaminants may cause effects (e.g. biological effects due to additivity or synergisms; or chemical effects due to the postulated "carrier effect" of one or more contaminants aiding the desorption of others) which cannot be managed one chemical at a time by numerical criteria.

This discussion leads to a third caveat. Although the flux data suggest that sediment contamination does not appear to prevent attainment of the few numerical water quality criteria that are available for organics, contaminated sediments in certain areas of the River do appear to pose a threat to living resources. Acute toxicity and a variety of chronic biological effects have been shown to be associated with whole sediments, either in solid phase bioassays or in situ (Alden and Young, 1982; Alden and Hall, 1984; Hargis et al., 1984; Weeks and Warinner, 1984, 1986; Pittinger et al., 1985; Weeks et al., 1986; Alden and Butt, 1987, 1988; Alden et al., 1988; and others). Attempts to manage contaminated sediments based solely upon their estimated potential for loading the water column with dissolved concentrations of contaminants that exceed numerical criteria would miss the major issue: sediments from certain areas of the Elizabeth appear to contain "toxics in toxic amounts". On the other hand, the flux equations could be employed as components of loading inventories established as integral parts of control strategies designed to limit the input of contaminants into the biologically active "reservoir" that the sediments clearly represent.

This page intentionally left blank.

SEDIMENT FLUXES OF METALS AND AMMONIUM

METHODS

Field and Laboratory Procedures

Benthic fluxes of metals and ammonium were determined using the procedures described by Burdige (1989), and are briefly described here. Sediments were collected on May 15, 1990 from sites EB, J, and M (see Figure 1; Table 9) utilizing the box corer described in the **Sediment Fluxes of Organic Contaminants: Methods** section. Modifications were made to this unit to include an acrylic chamber liner (16 x 22 x 33 cm), rather than the stainless steel liner and cylindrical glass insert used in the organics collection. The sediment depth within the acrylic liner ranged from 18 to 23 cm, with the overlying water varying from 10 to 15 cm in depth. Following retrieval of the box core assembly, the top and bottom of the liner were securely sealed with acrylic plates similar to those used to retain the organics core sample. The assembled flux chambers were submersed in coolers filled with bottom water taken from the site of collection in order to maintain the ambient temperature. Additional aliquots of bottom water were collected from each site for further use in the flux experiment. Upon return to the laboratory and throughout the duration of the experiments, samples were maintained at 20°C, a temperature very close to those observed in the field (Table 10). The overlying water of each chamber was carefully and thoroughly replaced with the additional bottom water collected at the same time as the

cores. Two cores each from Sites J and M and three cores from Site EB were utilized in the flux experiment. The extra core from Site EB was included due to the presence of live clams in this chamber.

A teflon stirrer assembly at the top of each chamber insured that a constant, gentle current was present in the aqueous phase, with comparable stirring rates in all chambers. The stirring was adjusted to reduce potential disturbance of the sediment phase surface. A 50 ml sample of the overlying water was withdrawn at 0, 1, 2, 4, 8, 16 and 32 hours subsequent to initiation of the flux experiment. An equivalent aliquot of the field collected, ambient bottom water was reintroduced into the chamber in order to maintain a constant aqueous phase volume. All water samples were filtered through a $0.45\mu\text{m}$ membrane and acidified (HCl for ammonium analysis; HNO_3 for metals analyses). Ammonium was determined by automated colorimetry and metals by flame or graphite furnace atomic absorption spectrophotometry (AAS). The AAS technique employed, the detection limits, and the quality control data for each elemental analysis are presented in Table 18. The detection limit for ammonium (NH_4^+) was determined to be 0.0056 mg/l.

Calculation of Flux Rates for Metals and Ammonium

The flux rate estimates were made by linear regression analyses of the change in concentrations of chemicals in the water column over time. The slopes of the regression equations represented the flux rates, while the standard errors of the slope coefficients were considered to be the error terms for the rates

Table 18. Analytical instrumentation, detection limits and Quality Control (QC) data for the metal analyses in the flux study.

<u>Metal</u>	<u>AAS Technique</u>	<u>Detection Limit ($\mu\text{g/l}$)</u>	<u>QC Data</u>	
			<u>Spike* Conc. ($\mu\text{g/l}$)</u>	<u>Percent Recovery</u>
Cadmium	Furnace	0.04	1.25	108
			1.00	79
Copper	Flame	1.00	5.00	115
			10.00	96
Iron	Flame	ND	50	110
			10	130
Manganese	Flame	20	5	120
			50	118
Nickel	Furnace	0.30	5.00	104
			10.00	96
Zinc	Flame	500	5	140
			50	96

*EPA QC Spikes used in the analyses.

observed for each chamber. The error terms for the site averages were calculated as the standard errors of the means of the replicate rate estimates. The flux rates were calculated both as a change in concentration ($\mu\text{mole}/\text{m}^2/\text{day}$; see Elderfield et al., 1981) as well as an areal loading rate (μg or $\text{mg}/\text{m}^2/\text{day}$).

Two other parameters (estimated doubling time; and percent change in ambient water concentrations introduced by the flux per day) were also calculated to indicate the magnitude of the flux rates relative to ambient concentrations in the water column. For the purposes of both of these calculations, a 5 meter depth was assumed and the time zero (0) water concentrations (C_w) were assumed to represent the ambient concentrations throughout the water column at the site. Doubling time was calculated by the following equation:

$$\text{Doubling Time (days)} = (C_{w(\text{time}0)} \times \text{Depth}) / (\text{Flux}) = \\ (\text{mg}/\text{m}^3) (\text{m}) / (\text{mg}/\text{m}^2/\text{day}). \quad [12]$$

The percent change calculations were as follows:

$$\% \text{ Change/day} = \text{Flux} / (C_{w(\text{time}0)} \times \text{Depth}) \times 100 = \\ (\text{mg}/\text{m}^2/\text{day}) / (\text{mg}/\text{m}^3) (\text{m}) \times 100. \quad [13]$$

The errors for these estimates were calculated by the following equation:

$$\text{S.E.}_x = \left(\left(\frac{\text{S.E.}_{C_w}}{C_w} \right)^2 X^2 + \left(\frac{\text{S.E.}_{\text{Flux}}}{\text{Flux}} \right)^2 X^2 \right)^{0.5} \quad [14]$$

where S.E. is the standard error for the associated term, X is either the doubling time or percent (%) change estimates, and the remaining terms are as above.

RESULTS AND DISCUSSION

Trace Metals

Percent recovery values ranged from 96-140% for the metals of interest (Table 18). Due to the consistently undetectable values for silver (Ag), arsenic (As) and lead (Pb), no sample computations were attempted for these elements.

Results from the flux computations are shown in Tables 19 and 20. Results for all fluxes were highly variable, although consistent trends were seen in the manganese (Mn) flux data. In several cases, the error ranges were greater than the means. This high variability is common in these types of measurements (Elderfield et al., 1981). The most significant finding determined was that, even with the data variability, most fluxes seem to be positive, indicating that the chamber sediments were releasing metals to the overlying water column phase.

An inter-site comparison indicated that no particular site demonstrated "across the board" patterns (i.e. either higher or lower rates for all contaminants) relative to the other sites. However, mean fluxes for Mn, nickel (Ni), and zinc (Zn) were greatest at Site EB. Site J exhibited the highest average fluxes for cadmium (Cd) and iron (Fe), although there was a high degree of variability between replicates (i.e. different flux directions) for these metals. Site M sediments displayed the highest flux rates for copper (Cu).

Table 19. Summary of Elizabeth River sediment flux studies for trace metals and ammonium fluxes. Values were calculated using the slope of the regression equation (regression coefficient) for each core chamber. Flux rates are reported in $\mu\text{mole/m/day}$. The error terms for each chamber represent the standard errors of the regression slopes, while those for the site averages are the standard errors of the means of the replicate rate estimates.

Site	Flux						
	Cadmium	Copper	Iron	Manganese	Nickel	Zinc	Ammonium
EB-A	0.11 ± 0.09	-98.0 ± 26.9	685 ± 122	113 ± 8.38	-11.3 ± 15.4	328 ± 124	4176 ± 544
EB-B	0.06 ± 0.11	6.98 ± 41.8	264 ± 40	143 ± 12.1	18.3 ± 8.9	645 ± 206	6344 ± 295
EB-C	0.34 ± 0.06	1.10 ± 4.49	2350 ± 201	130 ± 0.96	12.0 ± 5.9	243 ± 99	8870 ± 529
Average	0.17 ± 0.07	-30.0 ± 27.8	1100 ± 520	129 ± 7.09	6.33 ± 7.35	405 ± 100	6463 ± 1107
M-A	0.10 ± 0.43	7.44 ± 2.70	426 ± 74.7	112 ± 11.1	0.51 ± 0.28	207 ± 90.2	9595 ± 213
M-B	0.20 ± 0.25	6.25 ± 2.27	249 ± 343	83.0 ± 46.7	0.02 ± 0.20	186 ± 93.5	5302 ± 299
Average	0.15 ± 0.03	6.85 ± 0.42	338 ± 62.6	97.5 ± 10.2	0.26 ± 0.17	196 ± 7.42	7448 ± 1518
J-A	0.99 ± 0.23	0.17 ± 0.02	-55970 ± 267974	92.6 ± 5.84	-0.59 ± 1.02	18.4 ± 69.5	11.0 ± 216
J-B	-0.14 ± 0.17	0.21 ± 0.03	333790 ± 403954	86.6 ± 7.01	6.20 ± 3.36	-4.0 ± 213	2268 ± 169
Average	0.42 ± 0.40	0.19 ± 0.01	138910 ± 137801	89.6 ± 2.12	2.80 ± 2.40	7.2 ± 7.92	1139 ± 797
Summaries:							
EB	0.17 ± 0.07	-29.9 ± 27.8	1102 ± 520	129 ± 7.09	6.33 ± 7.35	405 ± 100	6463 ± 1107
M	0.15 ± 0.03	6.85 ± 0.42	338 ± 62.6	97.4 ± 10.2	26.3 ± 0.17	197 ± 7.42	7449 ± 1518
J	0.42 ± 0.04	0.19 ± 0.01	139160 ± 137801	89.6 ± 2.12	2.81 ± 2.40	7.2 ± 7.92	1139 ± 797

Note:

Positive fluxes indicate fluxes out of the sediments, while negative fluxes represent fluxes into the sediments.

Table 20. Summary of Elizabeth River sediment flux studies, trace metal and ammonium fluxes. Values were calculated using the slope of the regression equation (regression coefficient) for each core chamber. Flux data are reported in mass/m²/day. The error terms for each chamber represent the standard errors of the regression slopes, while those for the site averages are the standard errors of the means of the replicate rate estimates.

Site	Cadmium ($\mu\text{g}/\text{m}^2/\text{d}$)	Copper ($\mu\text{g}/\text{m}^2/\text{d}$)	Iron ($\text{mg}/\text{m}^2/\text{d}$)	Manganese ($\text{mg}/\text{m}^2/\text{d}$)	Nickel ($\mu\text{g}/\text{m}^2/\text{d}$)	Zinc ($\text{mg}/\text{m}^2/\text{d}$)
EB-A	12.45 \pm 10.22	-6222.14 \pm 1713.28	38.31 \pm 6.86	6.23 \pm 0.46	-663.05 \pm 906.49	21.43 \pm 8.13
EB-B	6.55 \pm 12.49	443.16 \pm 2654.69	14.79 \pm 2.26	7.83 \pm 0.67	1072.34 \pm 523.58	42.21 \pm 13.47
EB-C	37.99 \pm 7.38	70.00 \pm 285.15	131.45 \pm 11.25	7.14 \pm 0.52	705.58 \pm 345.52	15.91 \pm 6.51
Average	19.00 \pm 7.88	-1902.99 \pm 1765.48	61.52 \pm 29.08	7.07 \pm 0.38	371.62 \pm 431.16	26.52 \pm 6.54
M-A	11.00 \pm 48.27	472.77 \pm 171.34	23.82 \pm 4.17	6.14 \pm 0.61	29.71 \pm 16.97	13.53 \pm 5.92
M-B	22.21 \pm 28.44	396.90 \pm 143.84	13.90 \pm 19.21	4.56 \pm 2.56	1.14 \pm 11.80	12.18 \pm 6.13
Average	16.60 \pm 3.96	434.83 \pm 26.82	18.86 \pm 3.51	5.35 \pm 0.56	15.42 \pm 10.10	12.85 \pm 0.48
J-A	110.96 \pm 26.16	10.71 \pm 1.16	-3128.79 \pm 14980.00	5.08 \pm 0.32	-34.77 \pm 59.71	1.20 \pm 4.54
J-B	-16.18 \pm 18.65	13.60 \pm 1.88	18659.06 \pm 22580.97	4.75 \pm 0.38	364.19 \pm 196.90	-0.26 \pm 13.93
Average	47.39 \pm 44.95	12.15 \pm 1.02	7765.13 \pm 7703.17	4.91 \pm 0.12	164.71 \pm 141.05	0.47 \pm 0.52
Summaries:						
EB	19.00 \pm 7.88	-1902.99 \pm 1765.48	61.51 \pm 29.08	7.07 \pm 0.38	371.62 \pm 431.16	26.52 \pm 6.54
M	16.60 \pm 3.96	434.83 \pm 26.82	18.86 \pm 3.51	5.35 \pm 0.56	15.42 \pm 10.10	12.86 \pm 0.48
J	47.39 \pm 44.95	12.16 \pm 1.02	7765.14 \pm 7703.17	4.92 \pm 0.12	164.71 \pm 141.05	0.47 \pm 0.52

The variability in flux dynamics between site-metal combinations is not surprising due to the fact that there are multiple sources for these metals throughout the Elizabeth River system. Of the six metals evaluated in this study, Fe and Zn demonstrated the greatest average flux rates. Given the anoxic nature of the sediments, and the relative mobility and concentrations of these two metals, this is a logical and anticipated result.

The most consistent data were obtained for Mn fluxes, for which similar, positive fluxes were measured for all sites. Fluxes of Mn in the Elizabeth River sediments were at the low end of the extent of fluxes in Narragansett Bay sediments, where the values ranged from 120 to 870 $\mu\text{moles}/\text{m}^2/\text{day}$ (Elderfield et al., 1981).

Of the six metals of interest, average flux values for Cd varied the least from site to site. Elderfield et al. (1981) found that Cd flux values from Narragansett Bay sediments were low but within their limits of analytical precision (i.e. $0 \pm 0.004 \mu\text{moles}/\text{m}^2/\text{day}$). Average flux values for Cd from the Elizabeth River sites appeared to be up to two orders of magnitude greater than the Narragansett Bay upper limits. Fluxes for Ni from the Elizabeth River varied around the limits of $0 \pm 2 \mu\text{moles}/\text{m}^2/\text{day}$ determined for the Narragansett Bay sediments. Flux values for Cu were erratic, especially for Site EB where only one of the measured copper fluxes was negative. All other copper flux measurements were positive. These positive Cu fluxes again contrast with the study of Elderfield et al. (1981), where no fluxes or negative fluxes were

found. Similar studies in Narragansett Bay (Bender et al. 1978) found negative fluxes for Cd, Cu and Ni in comparable sediments.

The presence of seven soft-shelled clams was ascertained in flux chamber EB-C. It was postulated that this amount of living biomass would have a noticeable effect on the metal fluxes. There was an indication that Cd and Fe (and ammonium) fluxes were enhanced in this chamber, but no other metals seemed to be affected.

Average flux values for all metals at all sites, with only one exception, were positive, indicating that these sediments are acting as a source of metal contamination to the overlying water column. Tables 21 and 22 present the doubling time and daily percent change data for ambient water concentrations of metals. In general, the daily flux of metals represented 1-12% of the ambient load in the water column, producing doubling times between 8 and 86 days. However, two extreme values were also noted, a rapid replacement rate for iron in water for Site J (daily % change = 1258%; doubling time = 0.08 days) and a very low rate for zinc at the same site (daily % change = 0.1%; doubling time = 93 days). Considering the rather long residence time (1-2 months) of water in the River (Nielson, 1975), the modest positive flux rates of metals may be significant to the overall loading of the system. These rates should be assessed in the context of other point and nonpoint sources to the River. However, these values are very preliminary in nature, and may prove to be very different in magnitude for different regions and/or during different seasons. Further studies

Table 21. Doubling time (in days) of water column concentrations of trace metals and ammonium. Values are based on mean time zero (0) and mean flux data for each site. Each value represents the mean doubling time and standard error for each site. ND = Value not determined due to concentration of element below detection level at time 0.

Parameter	Site		
	EB	M	J
Cadmium	ND	157.8 ± 68.0	78.1 ± 74.1
Copper	6.1 ± 11.0*	ND	ND
Iron	8.1 ± 4.1	70.1 ± 13.1	0.08 ± 0.08
Manganese	65.1 ± 4.1	86.0 ± 9.1	62.6 ± 3.8
Nickel	8.5 ± 12.1	27.6 ± 61.2	32.2 ± 28.5
Zinc	12.8 ± 3.3	30.7 ± 4.0	936.0 ± 1043.1
Ammonium	17.4 ± 3.6	29.5 ± 13.1	63.0 ± 44.6

*Due to the fact that the copper flux at Site EB was negative (into the sediments), the value reported is actually the time required to decrease the water column concentration by 50%.

Table 22. Percent changes of trace metal/ammonium concentrations in the water column. Values are in percent per day. All calculations were based on mean time 0 and mean flux data for each site, as well as an assumed 5 meter water column height. Each value represents the mean percent change and standard error for each site. ND = Value not determined due to concentration of element below detection level at time 0.

Parameter	Site		
	EB	M	J
Cadmium	ND	0.6 ± 0.3	1.3 ± 1.2
Copper	-8.2 ± 14.9	ND	ND
Iron	12.4 ± 6.3	1.4 ± 0.3	1257.5 ± 1247.5
Manganese	1.5 ± 0.1	1.2 ± 0.1	1.6 ± 0.1
Nickel	11.7 ± 16.7	3.6 ± 8.0	1.6 ± 1.4
Zinc	7.8 ± 2.0	3.2 ± 0.4	0.1 ± 0.1
Ammonium	5.7 ± 1.2	3.4 ± 1.5	1.6 ± 1.1

are needed to confirm these findings, to determine seasonal variations in metal flux rates, and to determine the relation of these flux rates to pore water and sediment concentrations.

Ammonium

Fluxes of ammonium (defined here as ammonia-N + ammonium-N) measured at Sites EB, M, and J (Figure 1; Table 9) in May, 1990 ranged from 1139 to 7749 $\mu\text{moles N/m}^2/\text{day}$ (Tables 19 and 20). With the exception of the duplicate cores from Site J (in which core J-A appeared to show an anomalously low ammonium flux), there was good agreement between the ammonium fluxes determined in replicate cores from the other two sites. These fluxes are similar to those observed in other organic rich coastal and estuarine sediments (e.g., Elderfield et al., 1981; Klump and Martens, 1981; Boyton and Kemp, 1985; Burdige, 1989) including those at the Narragansett Bay sites where the previously discussed metal fluxes were also determined. These fluxes were most likely caused by the large concentration gradients in ammonium that exist across the sediment-water interface of these sediments.

Concentrations of ammonium in the pore waters of the upper 3 cm of these sediments ranged from approximately 1.2 to 8 mg N/l. Values in the water column at the time of these experiments were at least one order of magnitude lower (approx. 0.2 to 0.4 mg N/l), based on the ammonium concentrations measured in the waters overlying the cores or in the control flasks at the start of these experiments. The anoxic decomposition of organic matter in these

sediments (sulfate reduction), and the resulting ammonium production that occurs with this process, are the likely reason for the high pore water ammonium concentrations. Evidence for the occurrence of sulfate reduction in these sediments can be seen by the high levels of acid volatile sulfide (AVS) observed in the sediments from these sites (data to be reported in the ERLTM/M Annual Report to be submitted later).

It should be noted that the bottom oxygen measurements observed in the field at the time the cores were collected were still quite high (>6 mg/l). It is possible that low oxygen conditions typically observed in the Elizabeth River during the hot, late summer months may produce much higher ammonium flux rates. Indirect evidence has suggested that such conditions may introduce significant levels of ammonium to the waters of the Elizabeth River (Alden et al., 1987). Clearly, additional studies would be required to determine the relative loadings on a seasonal basis.